AAEC/E516

AAEC/E516

AUSTRALIAN ATOMIC ENERGY COMMISSION

RESEARCH ESTABLISHMENT

LUCAS HEIGHTS

HOT-WIRE ANEMOMETRY TECHNIQUES FOR AN AUTOMATED TURBULENCE MEASUREMENT RIG

by

J.D. HOOPER
R.W. HARRIS

March 1982

ISBN 0 642 59731 6

AUSTRALIAN ATOMIC ENERGY COMMISSION
RESEARCH ESTABLISHMENT
LUCAS HEIGHTS RESEARCH LABORATORIES

HOT-WIRE ANEMOMETRY TECHNIQUES FOR AN AUTOMATED TURBULENCE MEASUREMENT RIG

by

J.D. HOOPER
R.W. HARRIS

ABSTRACT

An automated rig has been constructed to allow continuous monitoring of the probe steady-state calibration during the measurement of the Reynolds stress tensor in turbulent single-phase flow using a two-channel hot-wire anemometer. The system consists of a signal switching and signal gain control unit, remote probe positioning along three coordinates, and a PDP11/10 computer for on-line data analysis. The system was calibrated using fully developed single-phase turbulent pipe flow; the results showed good agreement with published data. The calibrated system has been used to map the Reynolds stress field in three-dimensional duct flows having a similar turbulence level to developed pipe flow.

CONTENTS

(Continued)

1. INTRODUCTION

Turbulent single-phase flow is encountered in many engineering applications of fluid mechanics. Despite almost a century of scientific studies of the phenomenon and the associated development of predictive turbulence models, the approach remains largely empirical [Launder and Whitelaw 1977]. This is due partly to the nature of the equations of fluid motion (open and non-linear), and partly to the difficulty in accurately measuring parameters defining the random fluid motion.

The availability of large computing systems has led to the development of numerical models of turbulence capable of solving a truncated form of the fluid equations. By testing and refining such models against a wide range of experimentally known flows, it is hoped to formulate generalised predictive models of turbulence. The availability of experimental data on both the mean flow structure and such features of the turbulent flow as the Reynolds stress tensor is therefore important for understanding the physics of a particular flow, and obtaining data for use in the numerical procedures.

A major task for three-dimensional flow studies is the determination of the second-order moments of the fluctuating components of fluid velocity (the Reynolds stress tensor) and, perhaps, the higher order moments used for a kinetic energy balance. An automated turbulence measurement system, controlled by a PDP11/10 computer, has allowed the measurement of the turbulence structure of three-dimensional flow geometries within weeks rather than months. The system is also capable of continuously monitoring the probe and rig performance.

Many methods of measuring turbulence have been developed [Hinze 1975] but, at present, two techniques dominate the field. These entail the use of the constant temperature hot-wire anemometer and the laser-Doppler anemometer. Both instruments provide a signal that is proportional to the instantaneous fluid velocity resolved along one axis for a single point in the flow. The restricted nature of the information provided by such point probes requires excessive experimental time to map non-symmetrical duct flows, even for developed flow conditions. Flow visualisation studies, in which hydrogen bubbles or neutral density, micrometre size balls in water are illuminated in an intense narrow plane of light and sequentially photographed, should contain more detailed information. In one such study, a stroboscopic light source was used to investigate quantitatively the structure of the viscous sublayer

[Kutateladze et al. 1977]. The use of a computer to record and store this pictorial information can offer the experimenter a significantly more powerful tool for turbulent flow studies.

The two major advantages of laser-Doppler anemometry are the non-intrusive nature of the probe, and the linear relation of the output signal to the velocity component. It is superior to hot-wire anemometry for studies involving very high turbulence levels and a poorly known mean velocity direction. Disadvantages include the discontinuous nature of its output signal and the need to seed the flow with approximately 1 μm diameter reflecting particles. A further difficulty is determining the precise location of the measurement ellipsoid when the split laser beams pass through media of different refractive indices.

In a review of turbulence measurement systems, Launder and Whitelaw [1977] concluded that the use of hot-wire anemometry is justified for flows in which the turbulence level (u'/U) is less than 30 per cent. A study using a laser-Doppler anemometer to repeat data for an axisymmetric jet, a difficult geometry for the hot-wire anemometer, showed no discrepancy between the results of the two measurement systems [Reed et al. 1977].

The hot-wire anemometer has been in use for at least sixty years. It was operated initially in the constant current mode but, with the advent of high stability d.c. amplifiers, it is now operated in the constant temperature mode. Since they are subject to many sources of experimental error, hot-wire anemometer measurement systems should be tested in a known flow situation before any attempt is made to map an unknown flow geometry. For the present study, axisymmetric developed pipe flow was used for calibration.

2. HOT-WIRE ANEMOMETRY

2.1 Response Correlation of Hot-wire Element

The cooling of an internally heated slender cylinder, specified in terms of the Nusselt number (Nu) held at an angle α between the normal to the cylinder axis and an incident fluid of velocity U, has been defined as a function of the following dimensionless groups of physical parameters [Hinze 1975; Davies and Davis 1972; Bruun 1971a]:

$$Nu = f(Re, Pr, Gr, M, Kn, \ell/d_w, T_w/T_a, \alpha) \quad , \tag{2.1}$$

The Mach number (M) dependence is important for velocities in which compressibility effects occur ($U > 150$ m s^{-1} in air), and the Knudsen (Kn) effect has been shown [Davies and Davis 1972] to be significant only for conditions substantially below atmospheric pressure. In their investigation of the heat transfer from long slender cylinders in atmospheric pressure air flows, Collis and Williams [1959] revealed the limits of the free convection, mixed and forced convective heat transfer regimes. Their results showed that a 5 μm diameter wire was in the forced convective heat transfer region for $U >$ 0.10 m s^{-1}. They also found that for a wire Reynolds number of 44, which was independent of the incident-free stream turbulence intensity, the rate of heat transfer changed owing to vortex shedding. This wire Reynolds number corresponds to an incident velocity of approximately 130 m s^{-1} for a 5 μm diameter wire. For a constant temperature and density air stream and for the forced convective heat transfer region, the Grashof and Prandtl number dependence may be neglected.

2.1.1 Normal wire correlation

A theoretical evaluation of the relationship of the wire Nusselt number to the fluid Prandtl and wire Reynolds numbers [Hinze 1975] showed that for potential flow around a slender cylinder, the Nusselt number was given by

$$Nu = 1 + \sqrt{2\pi Pr\ Re} \quad . \tag{2.2}$$

Experiments have shown that the constants in the King's Law correlation (Equation 2.2) are untenable. However, many investigators have used the square-root relationship to the Reynolds number.

For a constant Prandtl number, and a flow normal to the wire axis, the hot-wire anemometer bridge voltage (E) is assumed to be related to the flow velocity, U, by

$$E^2 = A + B\ U^{0.5} \quad . \tag{2.3}$$

The constants A and B are determined experimentally, and are a function of the wire slenderness ratio (ℓ/d_w), the overheat ratio (T_w/T_a) and the wire material. A better approximation to the forced convective heat transfer region uses an index of 0.45 in Equation 2.3 [Collis and Williams 1959]; this

has been confirmed for velocities below 20 m s^{-1} [Bruun 1971a,b]. Siddall and Davies [1972] have shown that a fixed exponent correlation of the form of Equation 2.3 cannot represent the calibration curves over more than a limited velocity range; to extend the correlation to cover the wide velocity range 0.2 to 160 m s^{-1}, an empirical correction to the King's Law correlation was proposed, so that

$$E^2 = A + B\,U^{0.5} + CU \quad . \tag{2.4}$$

A generalised wire response has been shown to exist for a restricted range of probe element slenderness ratios, support prong geometries, wire overheat ratios and a fixed wire material [Davies and Davis 1972; Bruun 1971a; Bruun 1976a]. The response is presented in tabular form (Table A1) for a 2 mm long 5 μm diameter tungsten wire element, separated from the support forks by approximately 1.5 mm of copper plating, and operating at an overheat resistance ratio of 2.0. The probe was developed at the Institute of Sound and Vibration Research (ISVR), University of Southampton, UK. Any probe made from the same wire material and having the same nominal dimensions should be in fixed ratio to the standard probe response in the velocity range of the tabulation covering the forced convective heat transfer region between 0.2 and 150 m s^{-1}. The correlation used to fit the tabulated normal wire response was:

$$E^2 = E_o^2 + B\,U^n \quad . \tag{2.5}$$

The index n and variable B are velocity dependent, and are calculated by a piecewise expansion about the operating velocity.

The adoption of the standard probe geometry for most of the hot-wire probes constructed for the present study allowed the tabulated response to be tested extensively over the mean velocity range 4 to 30 m s^{-1}. The normal wire calibration curves for stable probes were in fixed ratio to the tabulated response. The use of the tabulated n index for the small-signal sensitivity considerably reduced the calibration time needed for new probe elements.

2.1.2 Inclined wire correlation

The response of a hot-wire element yawed at an angle α between the normal to the wire and the incident velocity U is, to a first approximation, sensitive only to the normal component U cos α. The cosine law breaks down

for large angles ($\alpha > 70°$) [Davies and Davis 1972]. Several modifications have been proposed to allow for the finite length of the wire, which causes the velocity component parallel to the wire to have some effect on the heat transfer. Champagne et al. [1967a,b] developed a correction to the cosine law in which the effective cooling velocity (U_e) is given by:

$$U_e = U (\cos^2 \alpha + k^2 \sin^2 \alpha)^{\frac{1}{2}} \quad . \tag{2.6}$$

The variable k is a function of the slenderness ratio of the wire. Friehe and Schwartz [1968] proposed an alternative equation for the yawed probe:

$$U_e = U [1 - k (1 - \sqrt{\cos \alpha})]^2 \quad , \tag{2.7}$$

where k is again dependent on the (ℓ/d_w) ratio for wire and thin film cylindrical probes. Kjellstrom and Hedberg [1968], using the correlation of Equation 2.6, found approximately the same dependence of k on the (ℓ/d_w) ratio, while other workers [Dean 1974; Bradshaw 1971] have supported the use of the cosine approximation for an effective yaw angle in the range 0 to 60°. The term 'effective yaw angle' is used, as inclined hot-wire elements are not straight lines and the effect of aerodynamic loading and thermal bowing may distort the wire even further. A modified cosine correlation was developed by Bruun and Davies [1969] in which the effective cooling velocity is given by:

$$U_e = U \cos^{m_1} \alpha \quad . \tag{2.8}$$

The correlation for a yawed wire then becomes:

$$E_\alpha^2 = E_o^2 + B U^n \cos^m \alpha \quad . \tag{2.9}$$

For the velocity range covered by Table A1, the difference (n-m) is approximately 0.05.

The use of the cosine law (Equation 2.9) significantly simplifies the expressions for the small-signal sensitivity of the wire when compared with the expansion developed from Equation 2.6.

The yawed wire correlation (Equation 2.9) was adopted in the present study. The effective wire angle, α, was found from six 'yaw up' and 'yaw down' measurements, in a uniform velocity low turbulence level flow using an

incremental angle δ of $\pm$ 2.5° and covering the range $\pm$ 15°. The calibration yaw box was placed at the entrance of the round duct and the effective angle measured at approximately the same mean velocity as the calibration study. Using Equation 2.10 to obtain twelve individual estimates of α, it was possible to define the effective probe angle to within a standard deviation of $\pm$ 0.5°.

The effective wire angle, α, can be found from:

$$\alpha = \left[\tan^{-1} \cot \beta - \operatorname{cosec} \beta \left(\frac{E_{\alpha+\beta}^2 - E_o^2}{E_\alpha^2 - E_o^2} \right)^{\frac{1}{m}} \right] , \qquad (2.10)$$

where β = experimental yaw angle, E_o = no flow voltage, and

$E_{\alpha+\beta}$ = voltage with yaw, E_α = voltage with no yaw.

The large errors indicated by Champagne and Sleicher [1967] and attributed to using the cosine law to evaluate the Reynolds stress components $-\rho \overline{uv}$ and $\rho \overline{v^2}$, were not apparent in the calibration pipe flow results. The fact that large errors were not observed may be due to the use of an effective wire angle which was not necessarily equal to the optically measured angle.

2.2 Anemometer Linearisation and Small-signal Sensitivity

The small-signal sensitivity of normal or yawed hot-wire elements may be derived directly from the small-signal expansion at the local mean velocity (Appendix B), or an analogue lineariser network can be used to give a constant small-signal sensitivity. For turbulence levels less than 18 per cent, the use of a lineariser for the measurement of the Reynolds stress tensor is no more accurate than the small-signal expansion of an accurately fitted correlation [Bruun 1971b, 1976b].

The ISVR hot-wire anemometer circuit [Davies and Mason 1974] is shown diagrammatically in Figure 1; two anemometers built by Communication Electronics (Southampton, UK) to this design were used. The lineariser network is an adjustable 10-point transistor function generator, approximating the inverse of the anemometer response curve of Figure 2 over the desired velocity range. Two d.c. coupled amplifiers (Figure 1) are needed to remove the no-flow bridge voltage and condition the signal in the pre-set 0 to 10 volt range. A small zero drift in either d.c. amplifier translates the

bridge voltage to an inappropriate section of the lineariser curve, introducing unknown errors in the results. For this reason the bridge signal output voltage was used.

A fundamental objection to the use of small-signal sensitivities derived from the steady state correlation has been made by Perry and Morrison [1971]; they showed an error of ± 20 per cent in the measurement of the axial turbulence intensity u' if the steady-state correlation was used, and advocated dynamic calibration. To achieve this, the probe was shaken mechanically by a linkage-generating sinusoidal motion, and the small-signal sensitivity derived direct from the known velocity perturbation in the constant air stream. Other workers have shown that static and dynamic calibrations give equivalent small-signal sensitivities, provided that the static calibration is accurately established [Bremhorst and Gilmore 1976; Bruun 1976a].

2.3 Probe Design and Calibration

A standard two-element hot-wire probe (Figure 3) was developed with the inclined wire centred on the probe axis. The offset distance of the normal wire from the probe axis was normally from 0.2 to 0.4 mm and, at the lowest distance, thermal wake interaction between the probe elements was negligible for velocities greater than 0.5 m s^{-1}. Thermal wake interaction effects can be large, particularly for in-line probe elements [Davies and Ko 1971]. The probe support forks are another important source of flow interference [Comte-Bellot and Strohl 1971, 1973] hence the probe design is arranged to minimise this effect. Rather than the standard X wire array, an asymmetric probe was adopted because of the difficulty in making a mechanically and electrically symmetrical pair of inclined wires on the same probe. This is necessary before the conventional signal sum and difference technique is used to obtain u and v.

The probe rotation scheme used during the measurements of the six terms of the Reynolds stress tensor is shown in Figure 4. One level of redundancy, as described in Appendix B, was allowed in the determination.

Operating the probe unattended over periods of 80 hours makes it difficult to monitor the drift in the probe calibration. Dust build-up on the probe is normally insignificant, because of the fine mesh filter at the blower inlet. One recommendation is to use dynamic calibration before and after each

experiment [Perry and Abel 1975], since there have been occasions when the small-signal sensitivity of the inclined wire changed in a stepwise fashion between calibrations. This was attributed to bowing, coupled with aerodynamic loads which strained the wire beyond the elastic limit during use, thus changing the effective wire angle.

Consequently, it is desirable for the wire calibration to be monitored continuously for both normal and inclined wires. This was achieved by using the anemometer bridge signal only for the Reynolds stress measurement. The mean velocity profile was determined by Pitot probes and stored in a computer file. Linear interpolation of the stored mean velocity radial traverse, appropriately scaled to ensure a constant Reynolds number, was used to set the mean axial velocity for the hot-wire probe. For constant atmospheric conditions, the ratio of the wire steady state voltage should be in a fixed ratio C to the standard probe response, so that

$$E_\alpha^2 - E_o^2 = C\, f(U) \cos^m\alpha \quad . \tag{2.11}$$

Equation 2.11 applies to both inclined and normal wires when α is equal to 0°. For stable probes, the proportionality value C held constant to within ± 5 per cent. Typical probe calibration curves are shown in Figures 5(a) and (b). Any drift in the wire performance could be readily detected, although rig air temperature changes altered E_o by approximately -2.5 mV/°C for a tungsten-wire probe. The rig temperature was also monitored so that the temperature effect could be compensated. The computed ratio C can also be used to allow a direct comparison of the signal variance recorded by a normal or inclined wire run at different over-heat ratios, or different probes with the same effective angle.

If Equation 2.11 or the tabulated standard response (Table A1) are generally applicable for all probes manufactured to a standard design, the ratio of the signal variances (e^2/C) should be equal for the same flow conditions. This is derived without the need for small-signal approximations, and Figures 6(a) and (b) show the results of running the same probe at three different overheat ratios for the same traverse and nominally the same flow conditions. The range of C values encountered in this test (1.057 to 0.651) exceeds the range of overheat ratios resulting from the 10 per cent spread of the cold resistance of probes operating at a constant hot resistance of 15 ohms.

The rig operating point, defined in terms of pressure, was calculated by scaling a reference static pressure (ΔP_r), air density (ρ_r) and kinetic viscosity (ν) by the appropriate ambient conditions; the rig Reynolds number was also held constant:

$$\Delta P = \Delta P_r \, (\rho/\rho_r) \, \left(\frac{\nu}{\nu_r}\right)^2 \quad . \tag{2.12}$$

The reference velocity profile was then scaled using Equation 2.13 to determine the mean velocity distribution:

$$U(r,\theta) = U_r(r,\theta) \, \left(\frac{\nu}{\nu_r}\right) \quad . \tag{2.13}$$

2.4 Closure of Small-signal Approximations

The a.c. component of the normal wire bridge voltage (e) has been shown (Appendix B) to be proportional, to first order, to the axial component of the fluid turbulence (u), as given by

$$u = e \, \frac{2 E U}{n(E^2 - E_o^2)}$$

$$= K_s \, e \quad . \tag{2.14}$$

The inclined wire bridge a.c. voltage, e_α, is similarly related to the axial and radial or azimuthal turbulence components by Equation 2.15:

$$\left(u + \frac{m}{n} \tan\alpha \, v\right) = e_\alpha \, \frac{2 E_\alpha U}{n \, (E_\alpha^2 - E_{o\alpha}^2)}$$

$$= K_\alpha \, e_\alpha \quad . \tag{2.15}$$

The use of the normal wire signal variance at rotation position 1, and the inclined wire signal variance at positions 1 to 6 as shown in Figure 4, allows the calculation of the Reynolds stress tensor.

It should be noted that the sign of the v component in Equation 2.15 is determined by the polarisation of the inclined wire by the turbulence structure near the wall; apparently there is, as yet, no explanation of this effect.

An additional equation is available if the cross product of the inclined and normal wire signal is time-averaged. This experimentally measured signal variance, $\overline{e\, e_\alpha}$, may then be compared with a calculated value (Equation 2.16):

$$P_{1,5} = \frac{\overline{e\, e_\alpha}_{1,5}}{\left[\frac{K_s}{K_\alpha}\overline{e^2} \pm \frac{K_\alpha}{4K_s}\left(\overline{e^2_{\alpha_5}} - \overline{e^2_{\alpha_1}}\right)\right]}, \qquad (2.16)$$

where P is the product ratio and the subscripts 1 and 5 for the ratio P and $\overline{e\, e_\alpha}$ refer to location 1 and 5 in the standard rotation system (Figure 4). The turbulent structure is independent of the arbitrary coordinate system used to resolve it, and the polar coordinate mesh is used only for convenience. This ratio is a general test of the small-signal approximations.

The computed cross product was compared with the experimental value in the r-z plane (locations 1 and 5), and the θ-z plane (locations 3 and 6), initially as a means of testing the spatial resolution of the hot-wire elements. The spatial averaging effect caused by the finite wire length in the measurement of frequency spectra has been considered [Wyngaard 1968], and it has been shown that turbulences with a length scale of the order of or less than the wire length are rapidly attenuated by spatial wire averaging. A similar analysis has been made for an X wire array using an assumed form of the frequency spectra [Bremhorst 1972].

A series of probes was made, each probe having a wire separation of between 0.2 and 1 mm; the computed and measured signal cross products were then compared. The results showed the ratio P to be unity, within the accuracy of measurement (Appendix C), as shown in Figures 7(a) to (d). This is to be expected if the small-signal approximations are accurate, for the spatial resolution of the wire should be at least equal to its constant temperature length which is approximately 60 per cent of the wire length or 1.2 mm. Alternatively, the measurement can be used to test the validity of the small-signal approximations in flow situations of increasing turbulence level. Measurement made downstream of a large blockage in an experimental rod bundle rig showed an increasing divergence of the P ratio from unity as the distance to the blockage decreased, indicating the technique to be a test of the accuracy of the first-order wire small-signal approximation.

3. DESIGN OF THE AUTOMATED RIG

A PDP11/10 computer, located in the AAEC's noise analysis laboratory at Lucas Heights, was used as the controller for the probe traverse and signal processing system. The general arrangement of the computer and attached peripherals is shown in Figure 8. A Hewlett-Packard model 3721A correlator and a Spectral Dynamics model SD 301B spectral analyser were interfaced with the computer, using special function subroutines written for the FOCAL language, under the locally developed operating system SAM2 [Harris 1975]. The four-channel analogue-to-digital converter (ADC) and the three-channel digital-to-analogue converter (DAC) were also controlled by the high level language FOCAL function subroutines. The noise analysis laboratory has the facility to process two analogue signals with a frequency range between d.c. and 20 kHz; this is the frequency band occupied by turbulence signals.

The control functions are:

(i) Motorised traverse with position feedback for (a) radial traverse, (b) azimuthal traverse, and (c) probe 270° rotation.
(ii) Signal line switching - any two of three analogue signals - to the noise laboratory.
(iii) Conversion of d.c. signal levels to a digital value using binary coded decimal (BCD) format at the rig without the need for intermediate d.c. coupled amplifiers.
(iv) Control of the blower to a computed set point.
(v) Minor control functions, such as switching on and off the teletype writer or RK05 disc drive unit to limit wear on these items.

A standard Digital Equipment Corporation foundation module, providing four sixteen-bit registers on the computer Unibus, was used to encode control signals which were routed to the remote decoder (Figure 5). The decoder was located at the rig. The bit pattern in the Unibus registers could be manipulated to allow the following functions [Harris et al. 1979]:

(i) Start a 3.5 digit panel meter (DPM) conversion, recognise finish and send BCD data to the PDP11/10.
(ii) Initiate drive for either of two stepping motors, by cyclically loading three bits through part of one register at the computer interface. An externally set interrupt was allowed for each drive.
(iii) Switch any combination of three analogue signal lines to the two

transmission lines to the noise analysis laboratory.

(iv) Switch eight relays singly or in pairs.

Two methods of motorised traverse were used; the first method employed pulse operated stepping motors (200 pulse/rev) for the radial and azimuthal traverse. A remote decoder initiated the pulse train which, when counted, allowed the probe position to be calculated from an initial reference point. Limit switches were set at the end of travel of the traverse gear to generate both an interrupt mode to the computer (soft limit) and disconnect the motor power supply to prevent probe damage (hard limit). The computer interrupt at the end limit allowed the creation of a reference point in the open loop position control system. In practice, correct adjustment of the geared traverse mechanism gave an accurate computed position without the use of this reference point.

A second method of position control is shown in Figure 9. This was a closed loop system, with the traverse position being calculated from the voltage read by an ADC channel connected to the wiper of a nominally linear potentiometer linked to the traverse mechanism. The error between the set and the required position controlled the raise or lower switching time for the traverse drive motor. It was not possible to use a simple proportional control system for the probe rotation servo-mechanism as a non-linear function of the position error had to be used to allow for the relay pick-up time and motor acceleration. A DAC channel was used to switch the motor drive control as there were no spare positions in the computer addressable registers to switch the relay drive amplifiers.

A similar system to that described above, but operating independently of the remote decoder unit, was used to provide a variable gain control for the two analogue signal lines connecting the rig to the noise analysis laboratory (Figure 10). An advantage of this general closed loop position control system is that any reversible d.c. or a.c. motor may be used as the actuating element. Two Princeton Applied Research Model 113 fixed gain signal conditioning amplifiers A1 and A2 (Figure 10) were used with the pass band set between 0.1 Hz and 100 kHz. The unity gain line driver, d.c. coupled amplifiers, built specifically for this rig, had an output impedance of 50 ohms and a flat frequency response to 20 kHz.

Although provision had been made for load control of the centrifugal blower powering the air rig, it was not required. The blower held to the set

pressure to within ± 1 per cent over extended operating periods. The longest unattended runs lasted 80 hours and generally were completed successfully.

4. ASYMMETRIC DEVELOPED TURBULENT SINGLE-PHASE PIPE FLOW

4.1 Experimental Rig

The pipe flow rig used for calibration was built from an aluminium tube (12.7 cm i.d. x 9.14 m long), with either a 45 or 26 kW centrifugal blower as the air supply unit. The calibration facility was made by a simple modification to the 6-rod subchannel test section [Hooper 1980].

Two 10 mm high internal pipe joining rings, 24 and 48 diameters from the entry, acted as unintended turbulence promoters. However, as the pipe was only 72 diameters long, this served to ensure developed flow conditions at the measurement plane, located 10 cm from the pipe exit. The computer operated probe traverse and rotation system developed for the subchannel test section (see Section 3) was available, together with the signal conditioning and on-line data processing, for measurements in the calibration pipe.

4.2 Mean Flow Results

The normalised mean velocity distribution, scanned radially across the pipe, is shown in Figure 11. It was measured by a 1.58 mm diameter Pitot probe with six 0.38 mm diameter static tappings, located 15 mm from the elliptical probe nose. The mean velocity was 11.6 m s^{-1}, corresponding to a Reynolds number of 86.5×10^3. Three traverses in the wall region ($y/R \leq 0.2$) were made to determine if the mean velocity profile changed in the wall region as the pipe exit was approached. The results at 10.0, 5.0 and 0.0 cm to the pipe exit plane were the same, within the estimated accuracy of measurement of the mean velocity, i.e. ± 1 per cent.

Two experimental methods were used to determine the local wall shear stress (τ_w) and friction velocity (v^*) for the developed flow region. The measurement of the axial static pressure gradient $\frac{\partial P}{\partial z}$ by a straight line fit, using a least squares method, to the somewhat arbitrarily selected developed flow region showed that all estimates were within an error range of ± 5 per cent.

$$\tau_w = \frac{\partial P}{\partial z} \cdot \frac{R}{2} \quad , \tag{4.1}$$

$$v^* = \sqrt{\frac{\tau_w}{\rho}} \quad , \tag{4.2}$$

where R is the pipe radius and ρ the air density.

The second method used a Preston tube, a square entry round tube located on the wall, to measure the total pressure. A range of Preston tube diameters, from 0.559 to 3.988 mm, was used to test the stated correlations of the Preston tube [Patel 1965] for both the transition region and turbulent core. These correlations were developed for a Reynolds number in the range 8.3×10^3 to 6.15×10^5 for axisymmetric pipe flow and boundary layers growing over flat plates. The Preston tube results were in good agreement with the static pressure determination of the wall shear stress, and had a standard deviation of ± 1.5 per cent for the range of probe diameters. Although only one Preston tube had the recommended internal to external diameter ratio of 0.60, the correlation showed that the reading was a function only of the probe external diameter for ratios above 0.17.

4.3 Turbulence Intensities and Reynolds Stresses $-\rho\,\overline{uv}$, $-\rho\,\overline{uw}$

The axial turbulence intensity u', normalised by the pipe wall friction velocity v^* for the 127.0 mm i.d. pipe is shown in Figure 12(a). The transverse intensities v' and w', and the Reynolds stresses $-\rho\,\overline{uv}$, $-\rho\,\overline{uw}$ are shown in Figures 12(b) to (e). The measurements were taken at an axial station 100 mm from the pipe exit. The results for the three probes A, B and C in measuring the axial turbulence intensity u' are generally consistent to within 6 per cent, or twice the standard deviation of the estimated accuracy of resolving u' (Appendix C). The results are in good agreement with those of other workers [Laufer 1954; Lawn 1971], and show greater consistency than the ± 10 per cent error (Appendix C).

The Reynolds stresses $-\rho\,\overline{uv}$ and $-\rho\,\overline{uw}$ are shown in Figures 12(d) and (e). The presence of a linear shear stress gradient for developed axisymmetric pipe flow in the r-z plane has been used by many workers as a calibration test for hot-wire anemometers. The distribution of the $-\rho\,\overline{uv}$ component of the Reynolds stress tensor may be derived from the axial momentum equation [Hinze 1975] which, for axisymmetric developed flow, reduces to equation 4.3:

$$0 = -\frac{\partial P}{\partial z} + \frac{\mu}{r}\frac{\partial}{\partial r}\left(r\frac{\partial U}{\partial r}\right) - \frac{\rho}{r}\frac{\partial}{\partial r}\left(r\,\overline{uv}\right) \quad , \tag{4.3}$$

Integration of Equation 4.3 with the boundary condition that at $r = R$ (the pipe wall), $-\rho\,\overline{uv} = 0$ (viscous sublayer) and $\frac{\partial P}{\partial z} \cdot \frac{R}{2}$ is equal to τ_w, or $\mu \frac{\partial U}{\partial r}\Big|_R$ lead to:

$$\frac{\partial P}{\partial z} \cdot \frac{r}{2} = \mu\frac{\partial U}{\partial r} - \rho\,\overline{uv} \quad . \tag{4.4}$$

If the viscous shear stress $\mu\frac{\partial U}{\partial r}$ may be neglected for the turbulent core region, the radial distribution of $-\rho\,\overline{uv}$ is linear, being zero at the pipe centre and becoming asymptotic to the wall shear stress. Several workers have used this distribution to evaluate the yawed hot-wire correlation [Kjellstrom and Hedberg 1968; Bruun and Davies 1969].

The shear stress in the r-z plane is consistent with the expected linear distribution to within 10 per cent. The axial symmetry of the pipe flow is demonstrated by the zero value of $-\rho\,\overline{uv}$ in the pipe centre. The magnitude of $-\rho\,\overline{uw}$ is approximately 0.1 τ_w over most of the pipe (Figure 12(e)). Although this is within the accuracy limits for a zero value, the data show a consistent non-zero value suggesting a systematic measurement error. This most probably is a result of the accuracy of the probe rotation system. Position 6 in the azimuthal plane corresponds to almost zero voltage on the reference potentiometer, making the location repeatable to only ± 3° compared to ± 1° for the other five locations.

5. CONCLUSIONS

Data from an automated turbulence measurement system for the determination of the Reynolds stress tensor by use of a two element hot-wire anemometer probe was in good agreement with published data for the calibration flow of axisymmetric developed single-phase turbulent pipe flow. The use of a standard probe geometry with support prongs well away from the 2 mm long active part of the hot-wire element allowed use of a standard probe response correlation, considerably simplifying the steady-state probe calibration. The adequacy of the probe small-signal approximations to the turbulent velocity fluctuations was experimentally tested and, for the turbulence levels present in the calibration pipe, were found to be accurate.

6. ACKNOWLEDGEMENTS

The work of Mr W.J. Crawford in the construction of electronic and mechanical components, and in the manufacture of hot-wire probes, is gratefully acknowledged. The work of Mr P. Ellis and his group in the AAEC Applied Physics Division in constructing the remote decoder unit and the PDP11/10 Unibus interface was of major importance to the development of the system.

7. REFERENCES

Bradshaw, P. [1971] - An introduction to turbulence and its measurement. Pergamon Press, Oxford.

Bremhorst, K. [1972] - The effect of wire length and separation on X array hot-wire anemometer measurements. IEEE Trans. Instrum. Meas., Vol. IM-21, No.3, p.244.

Bremhorst, K. and Gilmoree, D.B. [1976] - Comparison of dynamic and static hot-wire anemometer calibrations for velocity perturbation measurements. J. Phys. E. (Sci. Instrum.), Vol.9, p.1097.

Bruun, H. [1971a] - Interpretation of a hot-wire signal using a universal calibration law. J. Physics E. (Sci. Instrum.), Vol.4, p.225.

Bruun, H. [1971b] - Linearisation and hot-wire anemometry. J. Phys. E. (Sci. Instrum.) Vol.4, p.815.

Bruun, H. [1976a] - A note on the static and dynamic calibration of constant temperature hot-wire probes. J. Fluid Mech., Vol.76, p.145.

Bruun, H. [1976b] - A digital comparison of linear and non-linear hot wire data evaluation. J. Phys. E. (Sci. Instrum.) Vol.9, p.53.

Bruun, H. and Davies, P.O.A.L. [1969] - The performance of a yawed hot wire. ISVR Memorandum 284, University of Southampton.

Champagne, F.H., Sleicher, C.A. and Whermann, O.H. [1967] - Turbulence measurements with inclined hot wires. Part 1 - Heat transfer

measurements with inclined hot wires. J. Fluid Mech., Vol.28, No.1, p.153.

Champagne, F.H. and Sleicher, C.A. [1967] - Turbulence measurements with inclined hot wires. Part 2 - Hot-wire response equations. J. Fluid Mech., Vol.28, No.1, p.177.

Collis, D.C. and Williams, M.J. [1959] - Two-dimensional convection from heated wires at low Reynolds numbers. J. Fluid Mech. Vol.6, No.5, p.357.

Comte-Bellot, G. and Strohl, A. [1971] - On aerodynamic interference caused by single hot-wire probes. Trans. ASME, J. Appl. Mech., Vol.38E, p.767.

Comte-Bellot, G. and Strohl, A. [1973] - Aerodynamic effects due to configuration of X wire anemometers. Trans. ASME. J. Appl. Mech., Vol.40E, p.661.

Davies, P.O.A.L. and Ko, N.W.M. [1971] - Interference effects of hot wires. IEEE Trans. Instrum. Meas., Vol.20, p.76.

Davies, P.O.A.L. and Davis, M.R. [1972] - Factors influencing the heat transfer from cylindrical anemometer probes. Int. J. Heat Mass Transfer, Vol.15, p.1659.

Davies, P.O.A.L. and Mason, J. [1974] - The ISVR constant temperature hot-wire anemometer. ISVR Technical Report 66, Southampton University.

Dean, R.B. [1974] - An investigation of shear layer interaction in ducts and diffusers. Ph.D thesis, Imperial College, London University.

Friehe, C.A. and Schwarz, W.H. [1968] - Deviations from the cosine law for yawed cylindrical anemometer sensors. Trans. ASME, J. Appl. Mech., Vol.35E, p.655.

Harris, R.W. [1975] - 'SAM' and FOCAL.RTX for a PDP11 with a disc unit. Proc. Decus-Australia, August, p.24.

Harris, R.W., Hooper, J.D. and Milne, J.D. [1979] - Computer control of an experimental turbulence rig. Proc. Decus-Australia, August, p.1617.

Hinze, J.O. [1975] - Turbulence. McGraw-Hill (2nd ed.)

Hooper, J.D. [1980] - Developed single-phase turbulent flow through a square-pitch rod cluster. Nuc. Eng. Des., Vol.60, p.365.

Kjellstrom, B. and Hedberg, S. [1968] - Turbulence measurements in a circular channel for testing hot-wire anemometer measurement techniques and evaluation methods. Atkiebolaget Atomenergi Report AE-RTL-1001.

Kutateladze, S., Khabakhapasheva, E.M., Orlov, V.V., Perpelitsa, V.B. and Mikhailova, E.S. [1977] - Experimental investigation of the structure of the near-wall turbulence and the viscous sublayer. 1st Int. Symp. on Turbulent Shear Flows, Pennsylvania, USA, April.

Launder, B.E. and Whitelaw, J.H. [1977] - Turbulent flow modelling. HTFS Design Report DR.44.

Lawn, C.J. [1971] - The determination of the rate of dissipation in turbulent pipe flow. J. Fluid Mech., Vol.48, No.3, p.477.

Laufer, J. [1954] - The structure of turbulence in fully developed pipe flow. NACA Report 1174.

Patel, V.C. [1965] - Calibration of the Preston tube and limitations on its use in pressure gradients. J. Fluid Mech., Vol.23, No.1, p.185.

Perry, A.E. and Morrison, G.L. [1971] - Static and dynamic calibration of constant temperature hot-wire systems. J. Fluid Mech., Vol.47, No.4, p.765.

Perry, A.E. and Abell, C.J. [1975] - Scaling laws for pipe flow turbulence. J. Fluid Mech., Vol.67, No.2, p.257.

Reed, X.B., Spiegel, L. and Harland, S. [1977] - Some measurements of spatial correlations in an axisymmetric turbulent jet. 1st Int. Symp. on Turbulent Shear Flows, Pennsylvania, USA, April.

Siddall, R.G. and Davies, T.W. [1972] - An improved response equation for hot-wire anemometry. Int. J. Heat Mass Transfer, Vol.15, p.367.

Wyngaard, J.C. [1968] - Measurements of small-scale turbulence structure with hot wires. J. Phys. E. (Sci. Instrum.), Vol.1, p.1105.

8. NOTATION

Re	Reynolds number
Pr	Prandtl number
Gr	Grashof number
M	Mach number
Kn	Knudsen number
K_s	Normal wire sensitivity
K_α	Inclined wire sensitivity
ℓ	Length of wire
d_w	Diameter of wire
T_w	Temperature of wire
T_a	Ambient temperature
α	Angle of inclined wire
E	Anemometer mean bridge voltage
e	Anemometer fluctuating bridge voltage
V	Mean velocity vector (components U,V,W with reference to polar coordinates z,r,)
u,v,w	Fluctuating components of velocity vector
n	Index in hot-wire response correlation
m	Index in yawed hot-wire response correlation
m_1	Index in yawed hot-wire response equation
P	Product ratio ($\overline{e_\alpha e}$), or static pressure
A	Constant in hot-wire response correlation
B	Constant in hot-wire response correlation
C	Constant in hot-wire response correlation or ratio to standard calibration curve

Subscripts

o	No flow valve
α	Inclined wire valve
e	Effective cooling velocity

Superscripts

$\overline{\quad}$	Time average quantity
*	Friction velocity
'	r.m.s. quantity

Greek symbols

ρ	Air density
ν	Air kinematic viscosity
τ_w	Wall shear stress

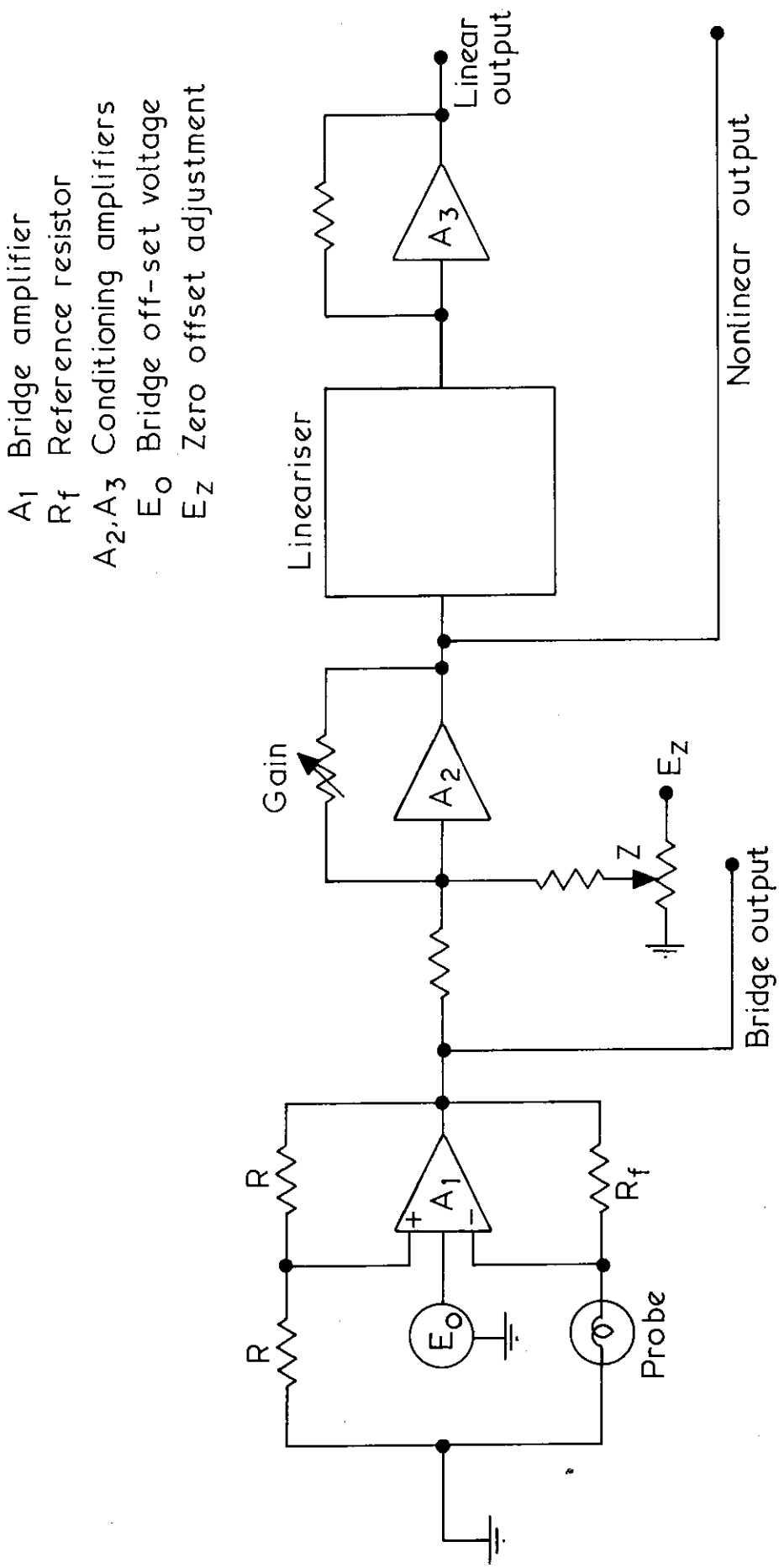

FIGURE 1. CIRCUIT OF ISVR HOT-WIRE ANEMOMETER

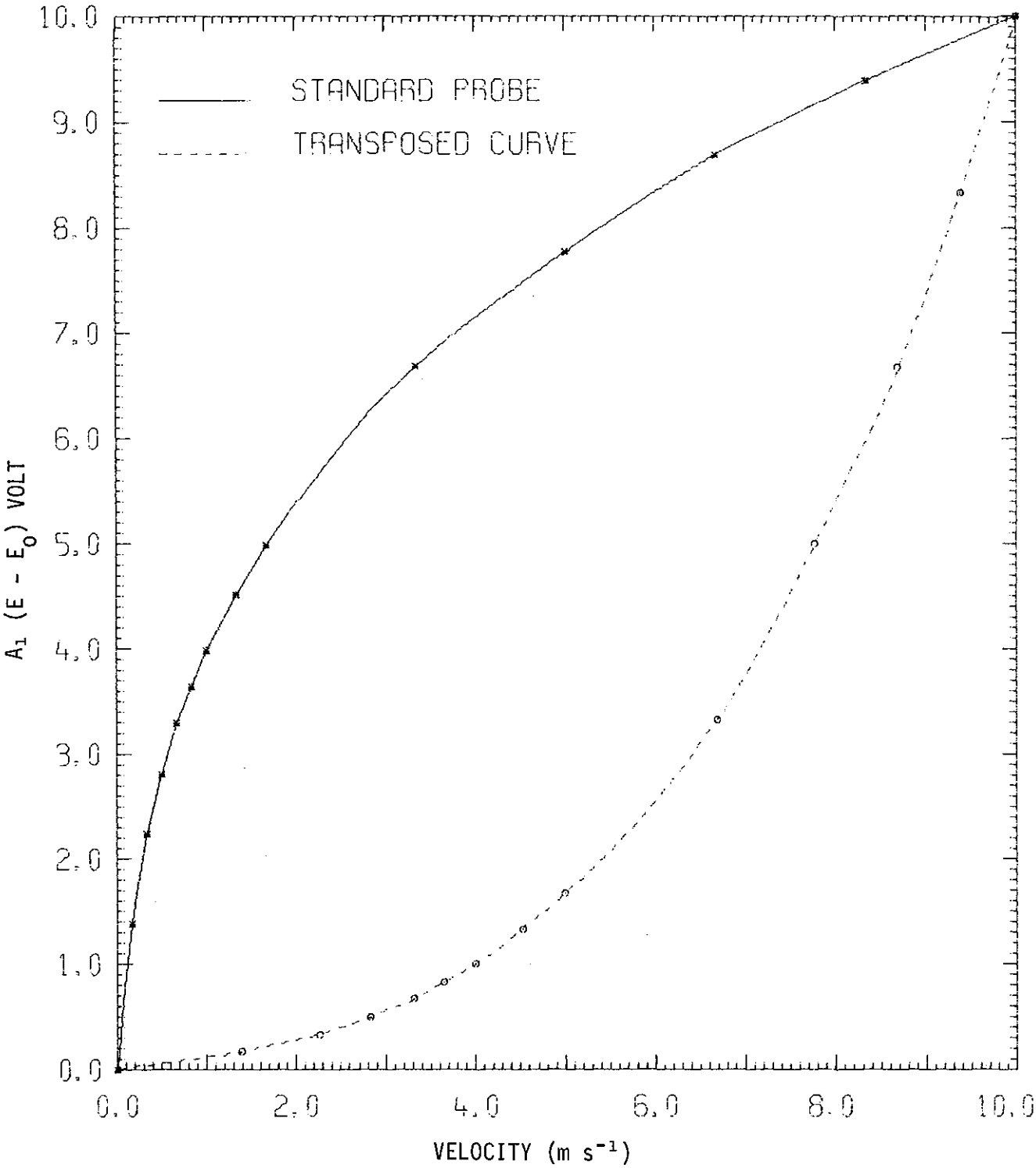

FIGURE 2. GENERAL HOT-WIRE PROBE RESPONSE AND LINEARISER CHARACTERISTIC

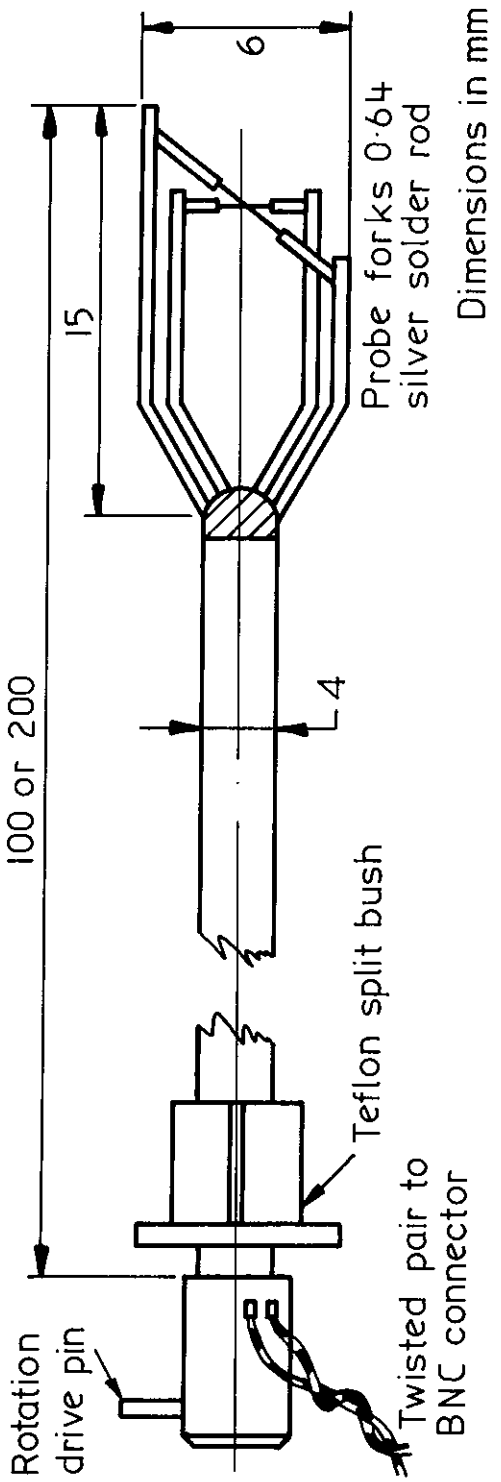

FIGURE 3. STANDARD HOT-WIRE PROBE DESIGN

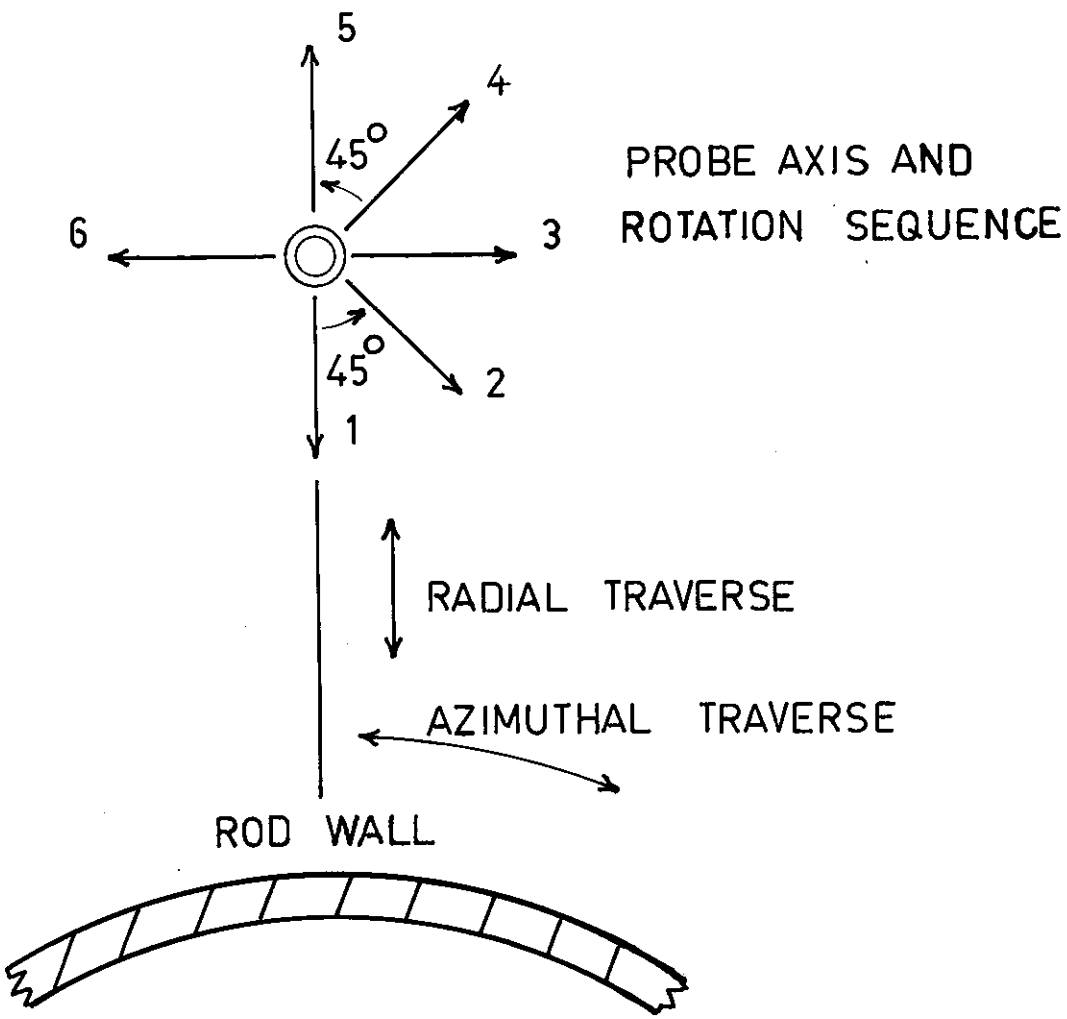

FIGURE 4. PROBE ROTATION SEQUENCE

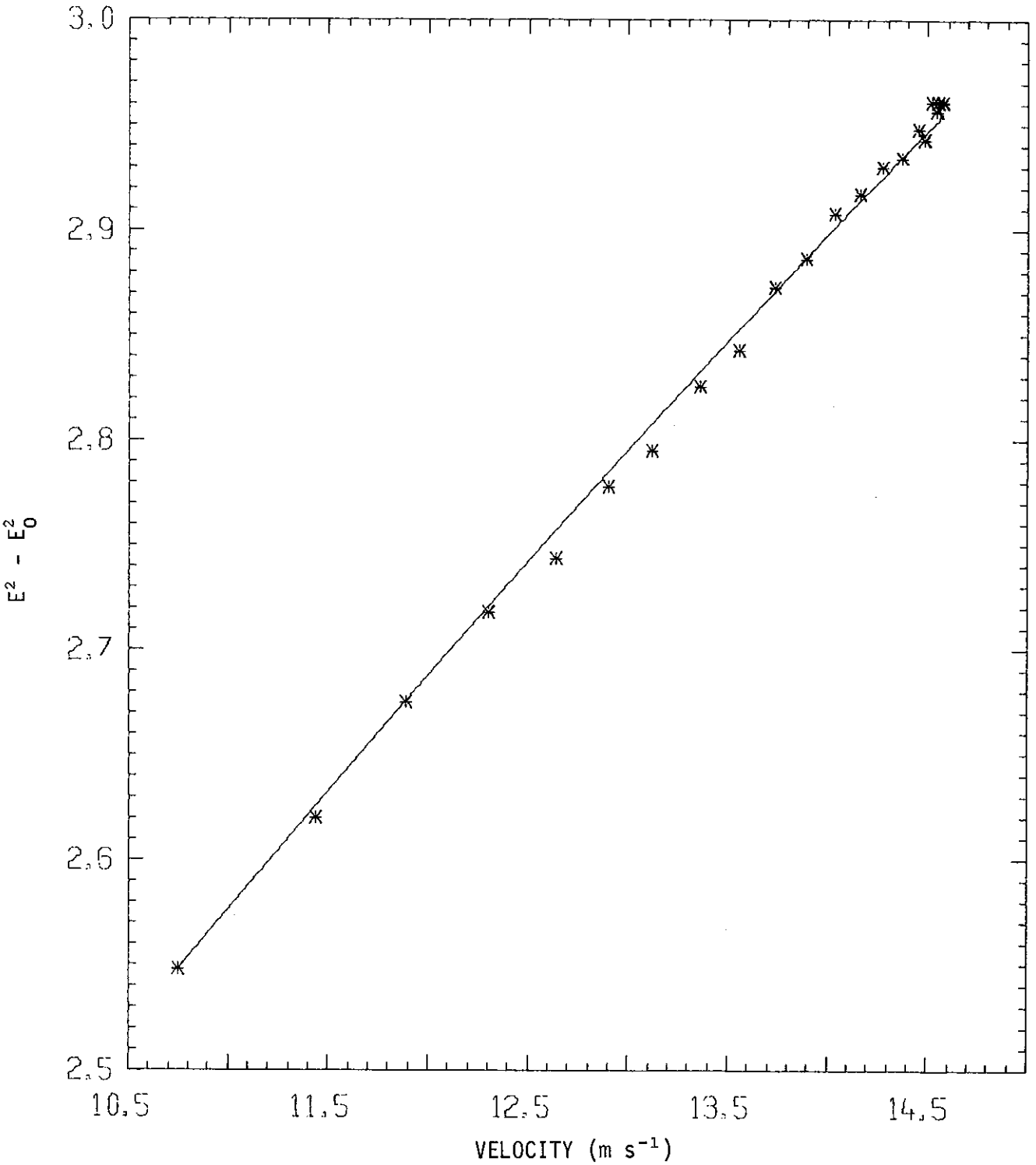

FIGURE 5(a). CALIBRATION CURVE OF NORMAL WIRE

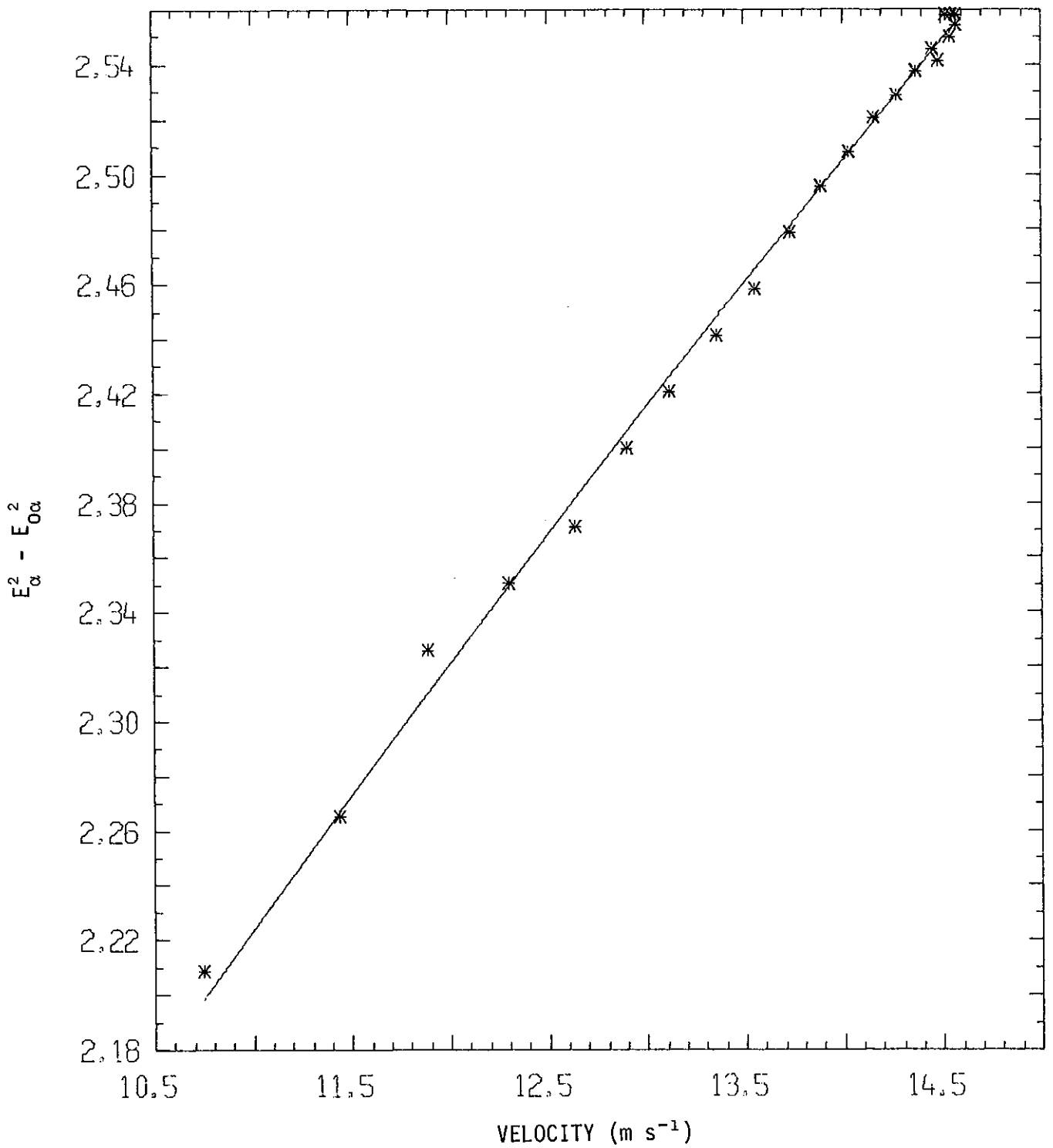

FIGURE 5(b). CALIBRATION CURVE OF INCLINED WIRE

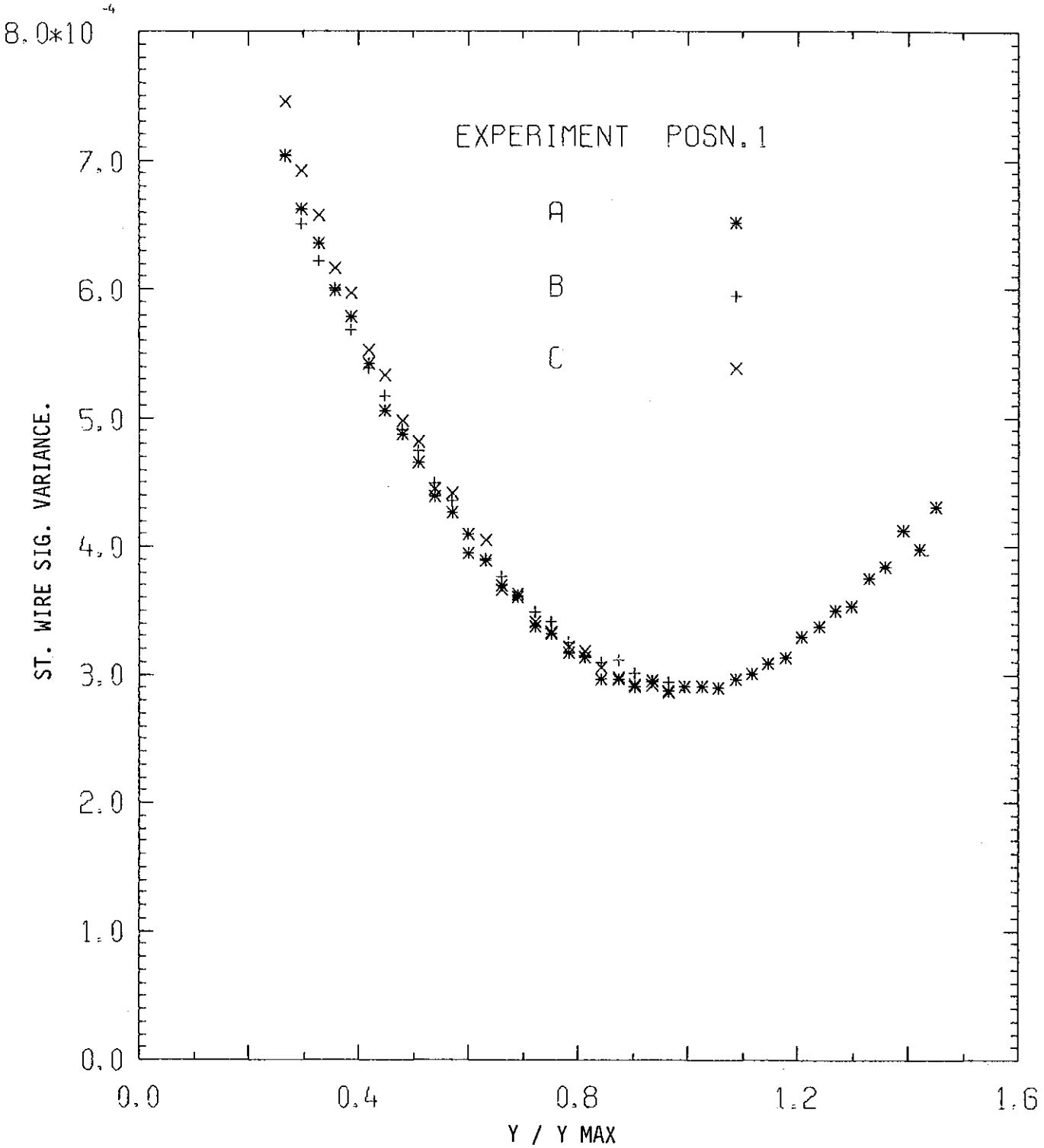

FIGURE 6(a). NORMAL WIRE PROBE RUN AT THREE OVERHEAT RATIOS: C RATIO A 1.057, B 0.983, C 0.783

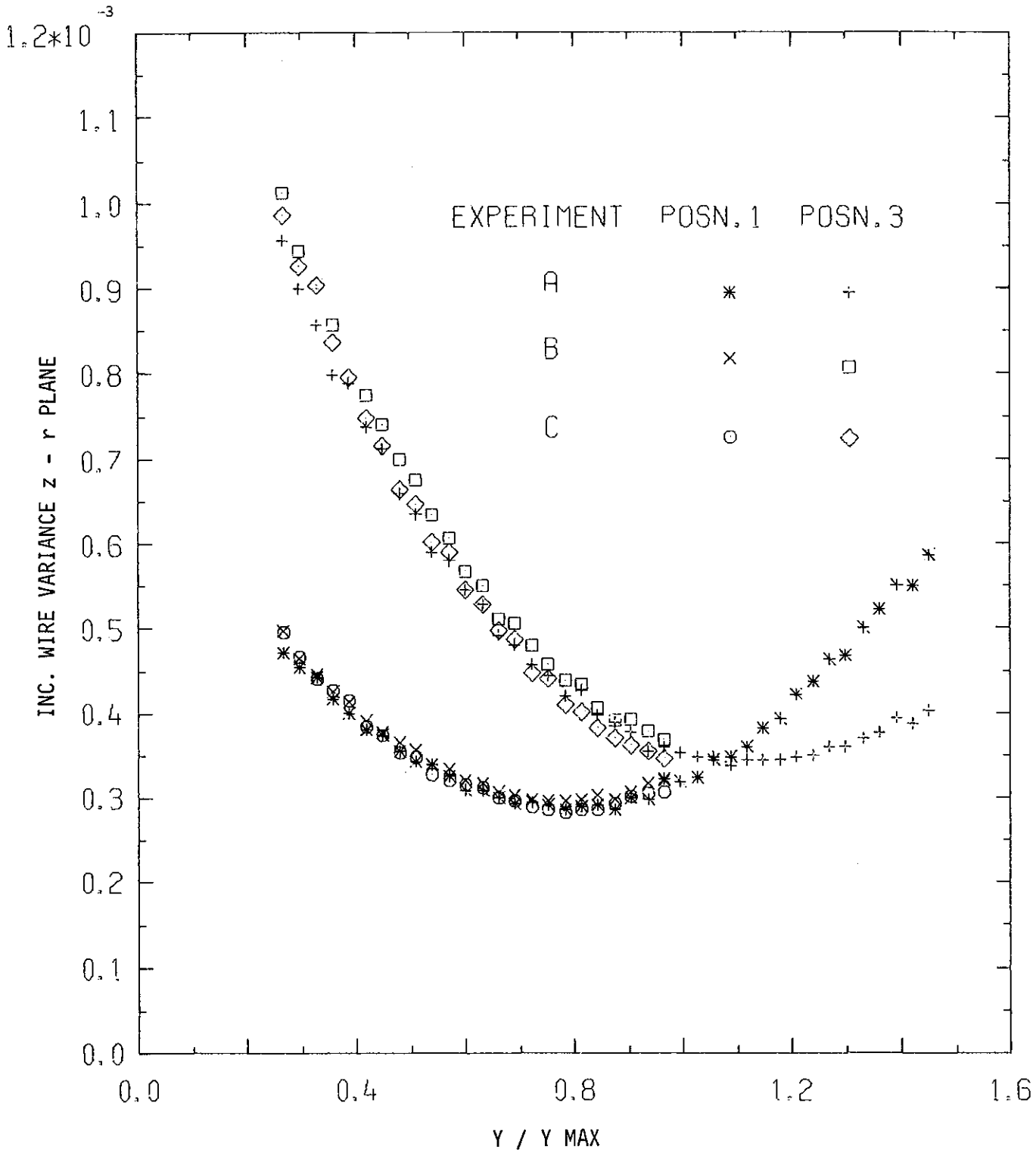

FIGURE 6(b). INCLINED WIRE PROBE RUN AT THREE OVERHEAT RATIOS: C RATIO A 0.985, B 0.651, C 0.894

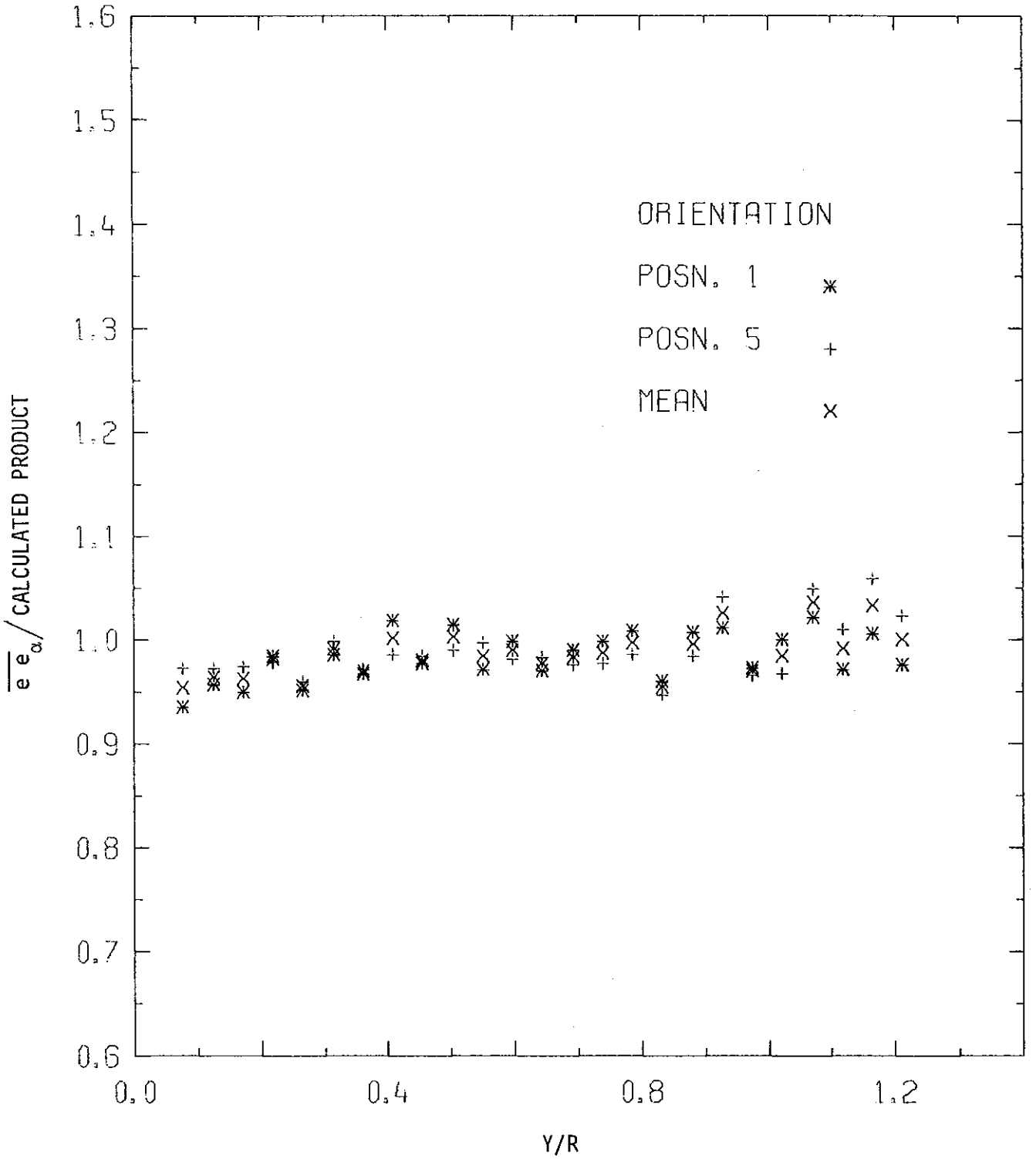

FIGURE 7(a). MEASURED TO COMPUTED CROSS-PRODUCT RATIO $\overline{e\,e_\alpha}$, WIRE SEPARATION 0.4 mm, r-z PLANE

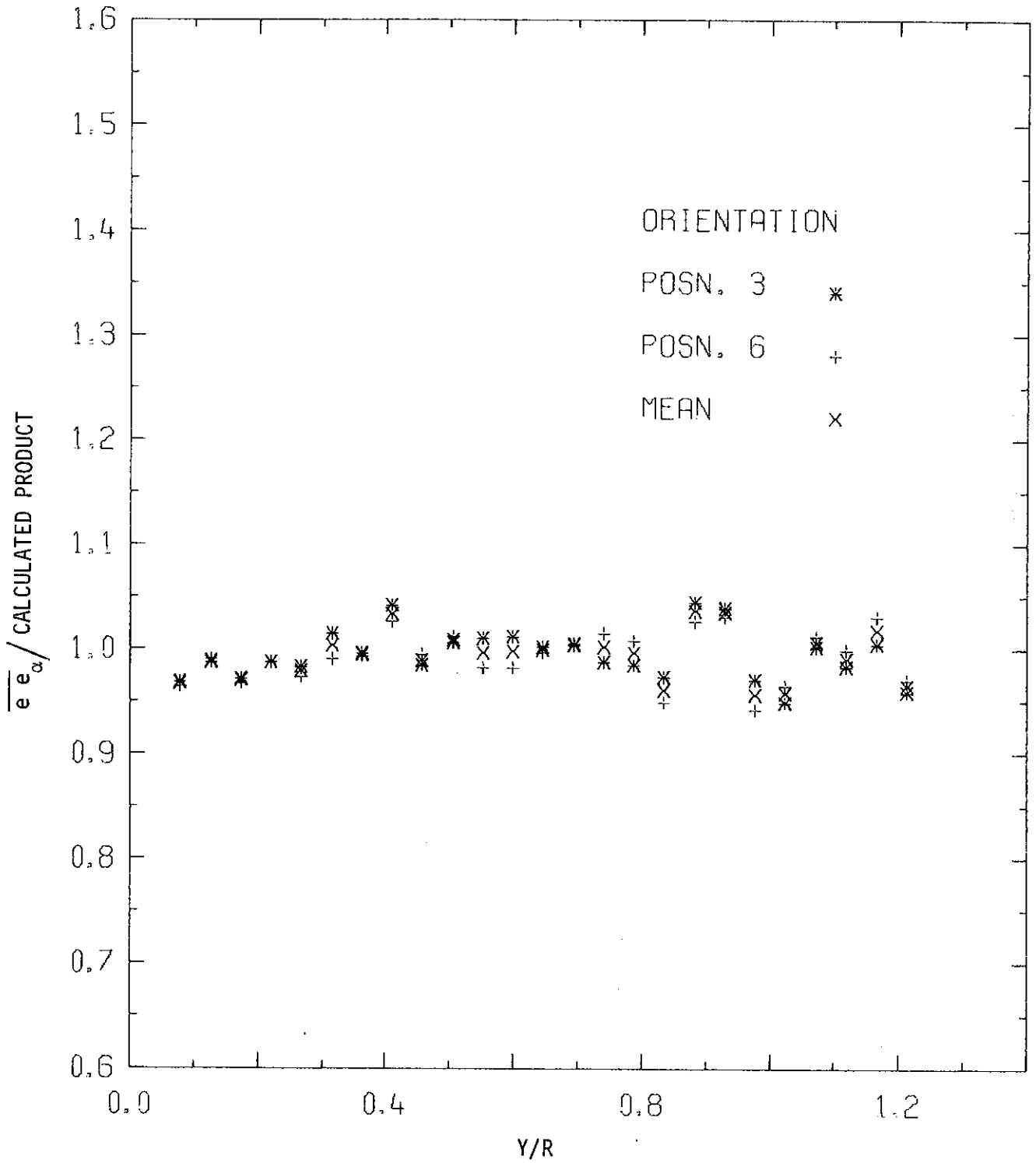

FIGURE 7(b). MEASURED TO COMPUTED CROSS-PRODUCT RATIO $\overline{e\,e_\alpha}$, WIRE SEPARATION 0.4 mm, θ-z PLANE

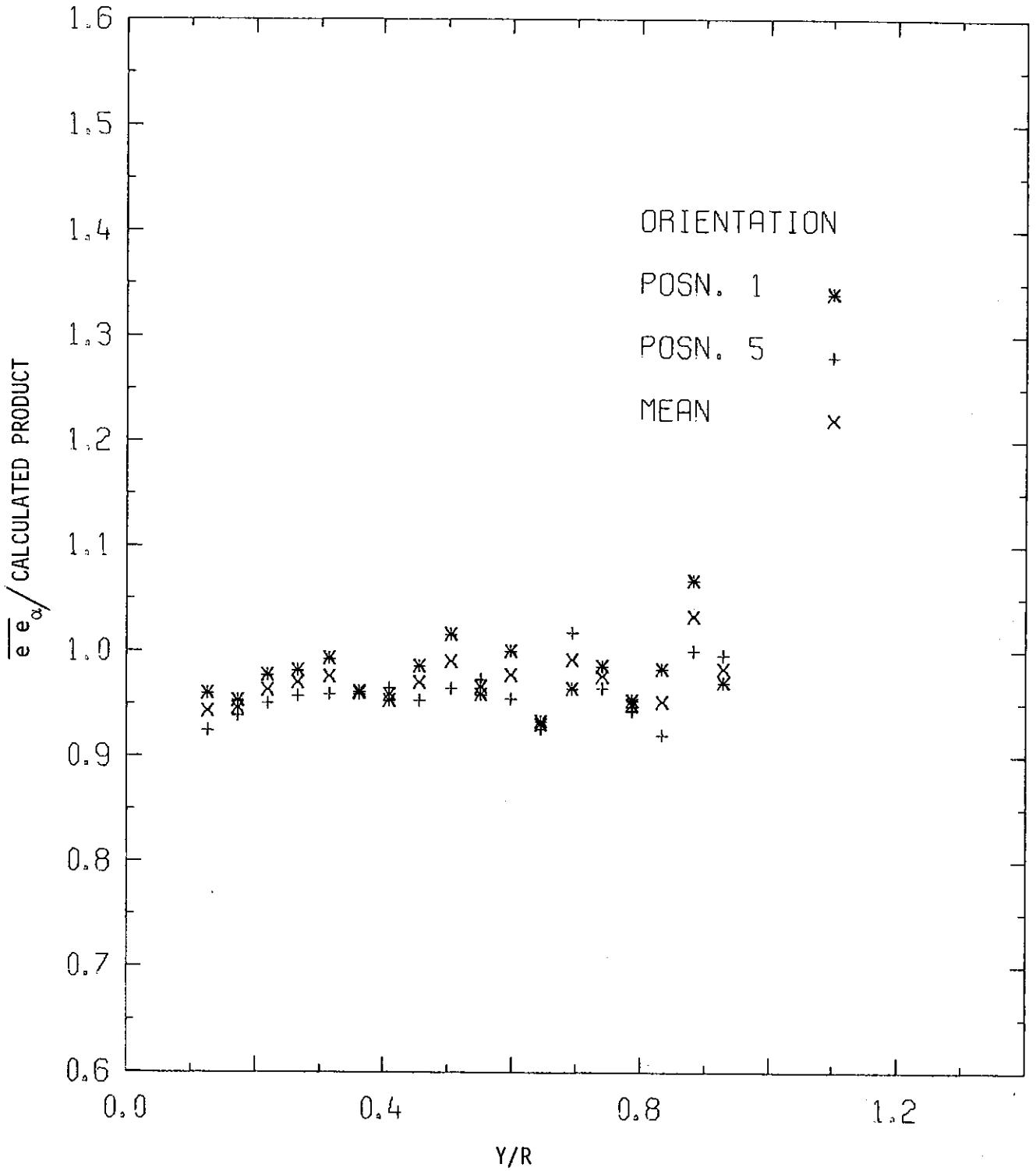

FIGURE 7(c). MEASURED TO COMPUTED CROSS-PRODUCT RATIO $\overline{e\,e_\alpha}$, WIRE SEPARATION 1.0 mm, r-z PLANE

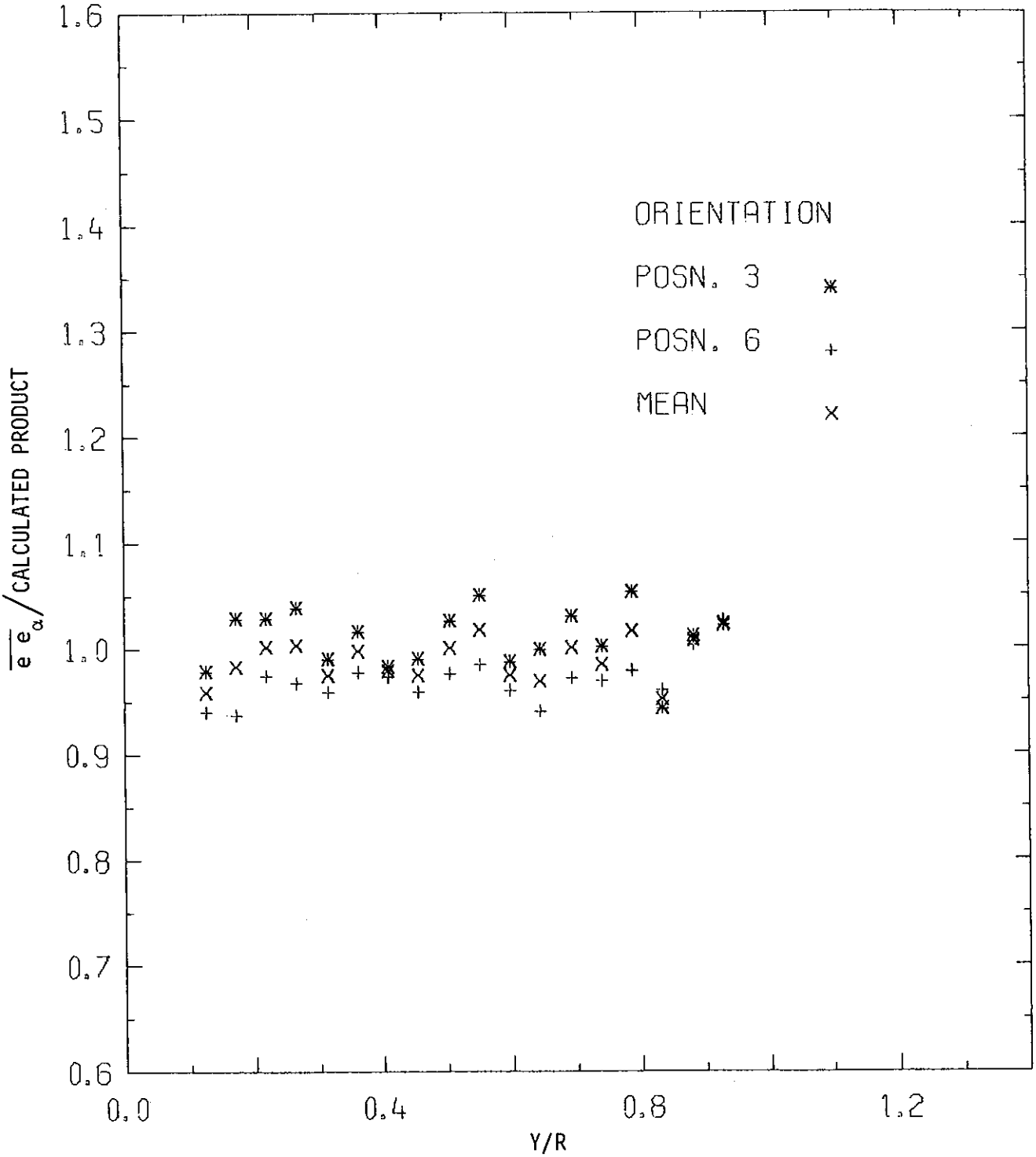

FIGURE 7(d). MEASURED TO COMPUTED CROSS-PRODUCT RATIO $\overline{e\,e_\alpha}$, WIRE SEPARATION 1.0 mm, θ-z PLANE

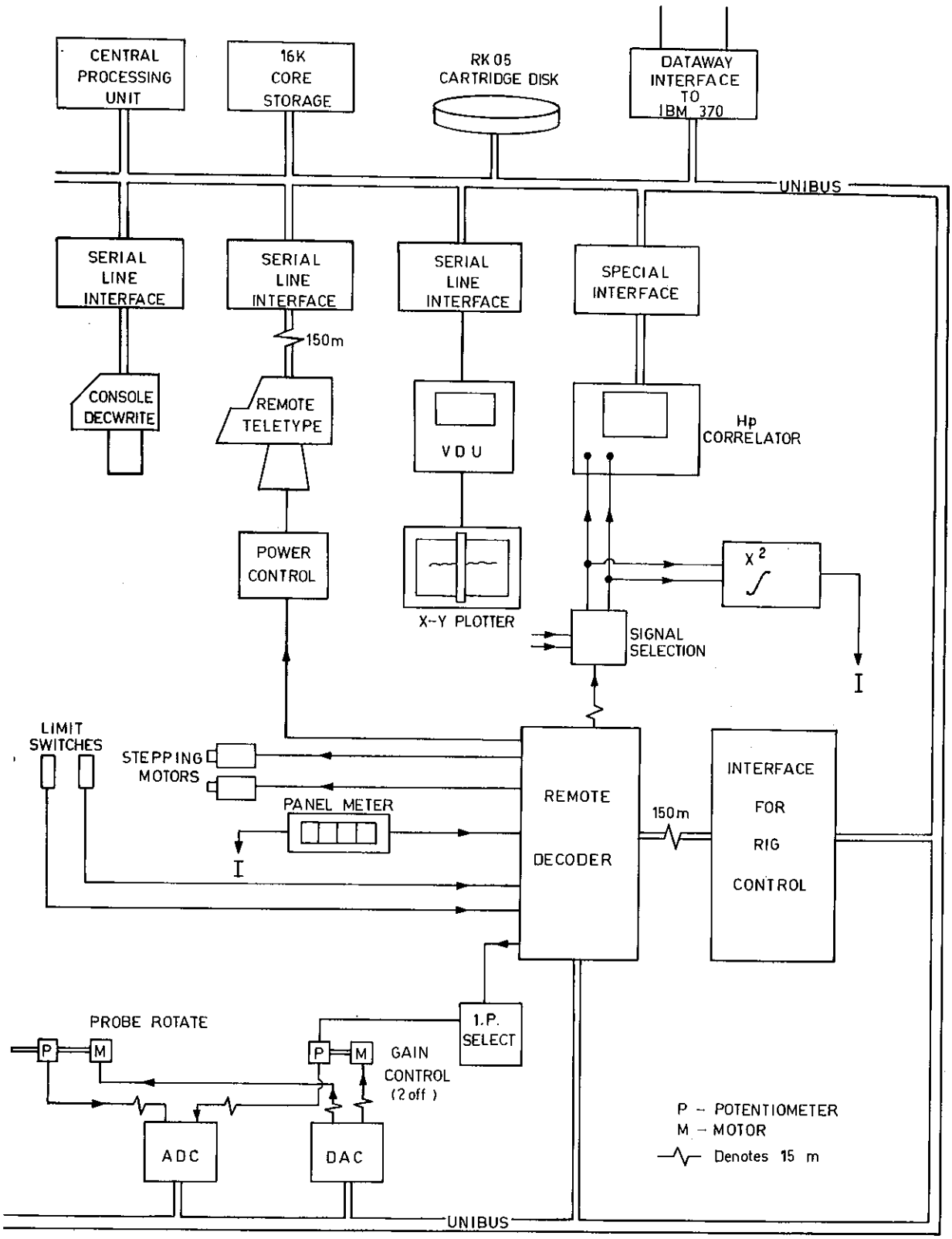

SCHEMATIC OF PDP 11/10 SYSTEM AND ASSOCIATED HARDWARE USED FOR AUTOMATIC CONTROL SYSTEM

FIGURE 8. ARRANGEMENT OF NOISE LABORATORY COMPUTER AND PERIPHERAL INSTRUMENTS

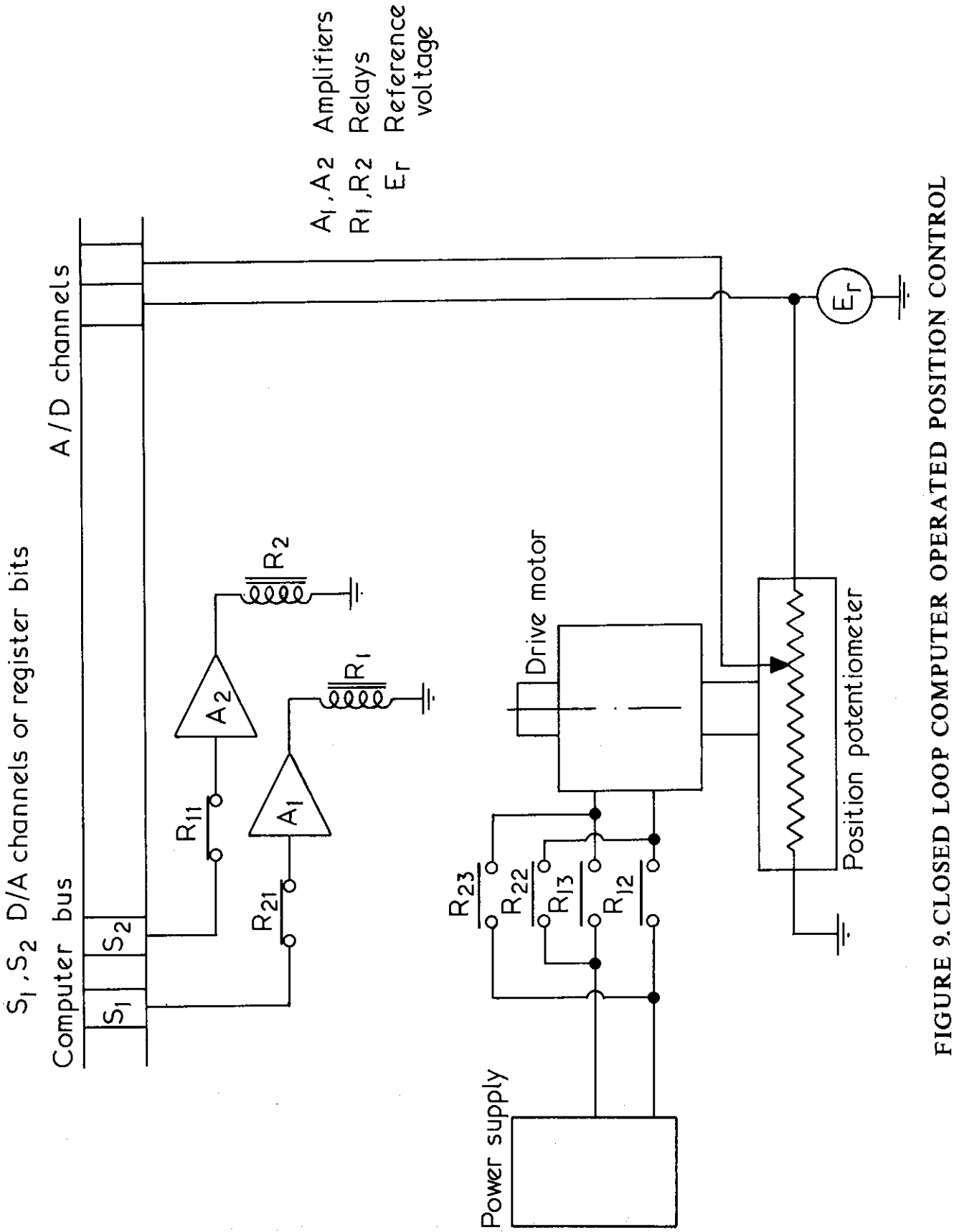

FIGURE 9. CLOSED LOOP COMPUTER OPERATED POSITION CONTROL

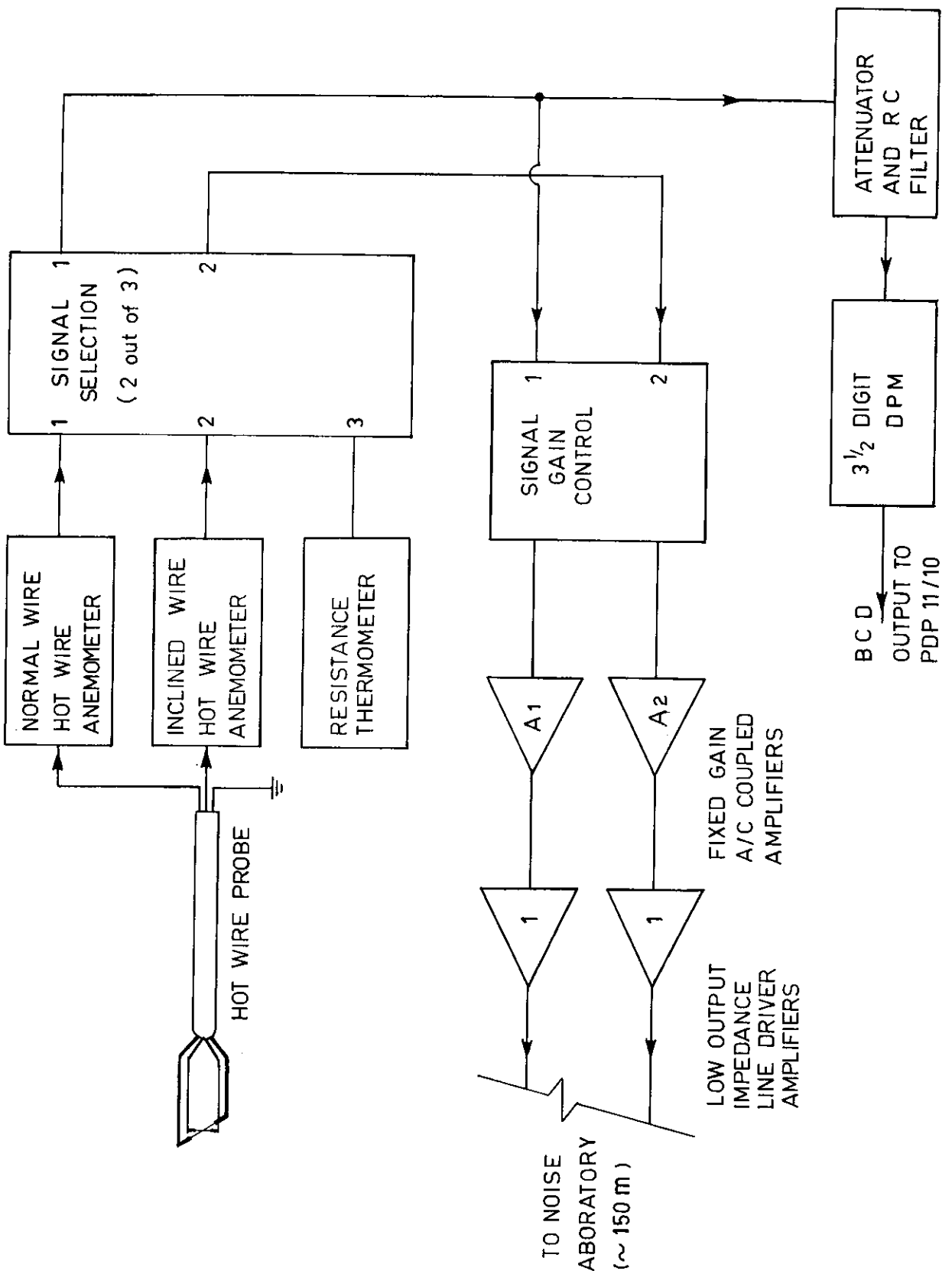

FIGURE 10. HOT-WIRE ANEMOMETER SIGNAL PROCESSING AT RIG

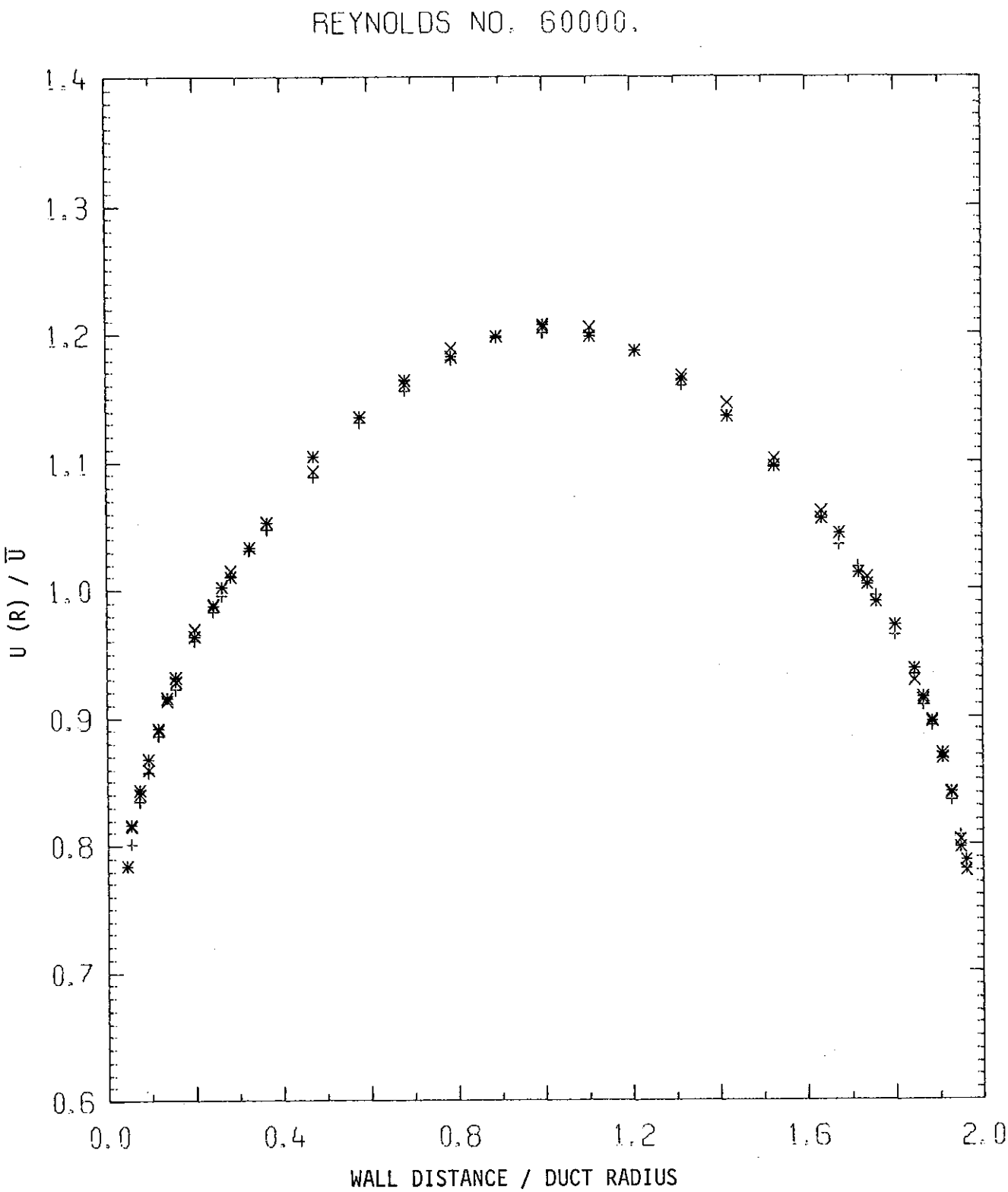

FIGURE 11. MEAN VELOCITY PROFILE, CALIBRATION PIPE 1

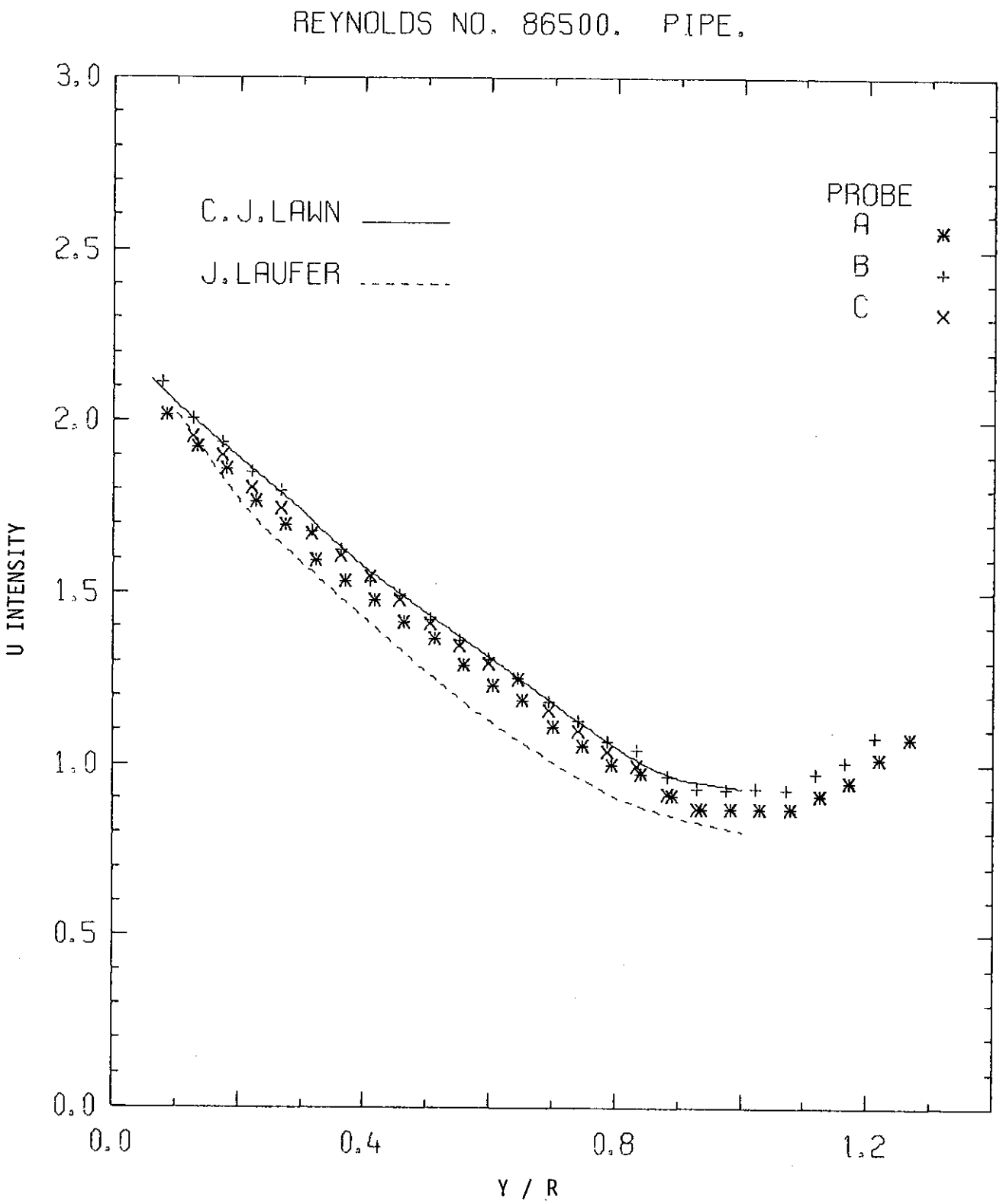

FIGURE 12(a). AXIAL TURBULENCE INTENSITY, CALIBRATION PIPE 2

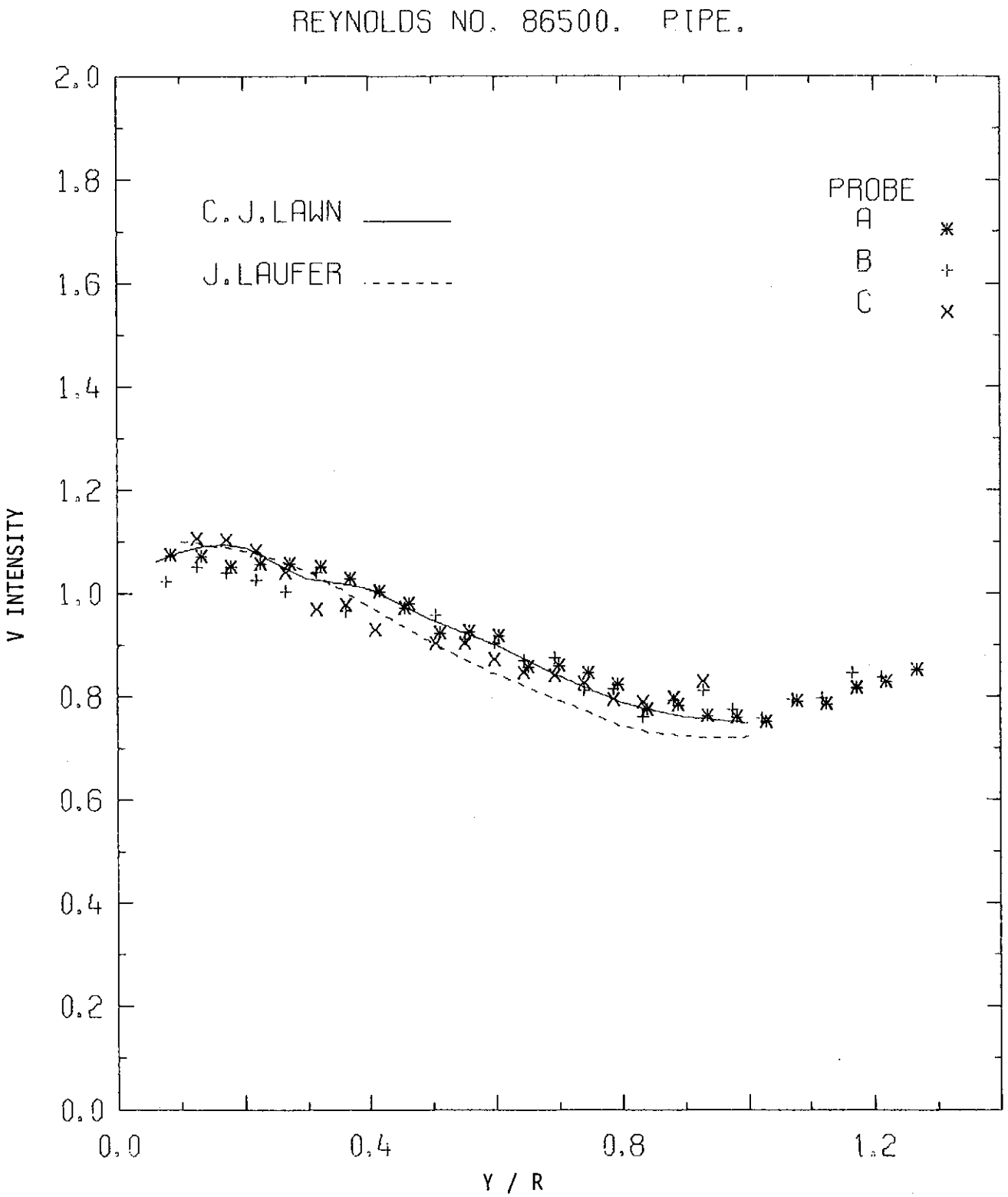

FIGURE 12(b). RADIAL TURBULENCE INTENSITY, CALIBRATION PIPE 2

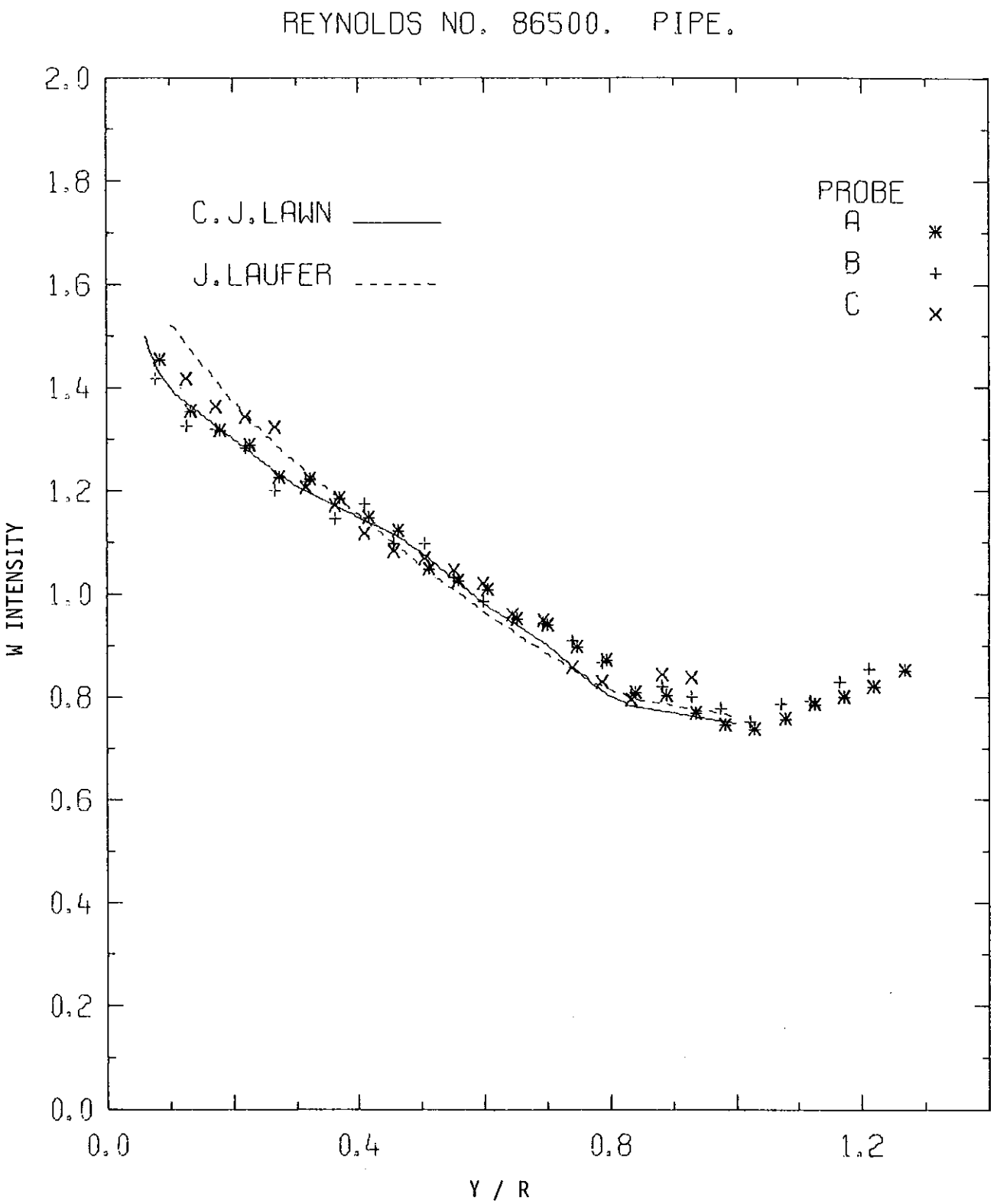

FIGURE 12(c). AZIMUTHAL TURBULENCE INTENSITY, CALIBRATION PIPE 2

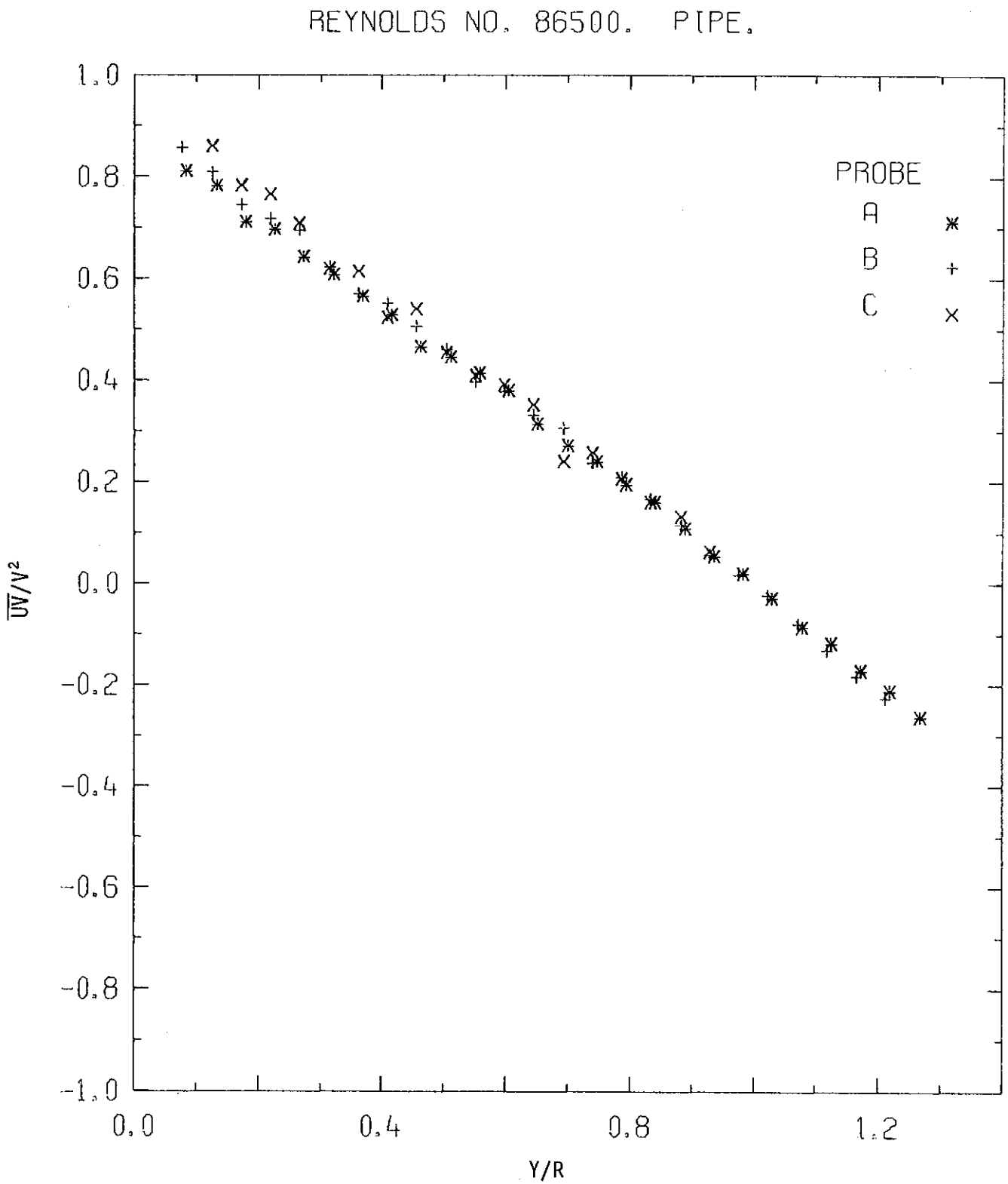

FIGURE 12(d). RADIAL COMPONENT OF REYNOLDS SHEAR STRESS, CALIBRATION PIPE 2

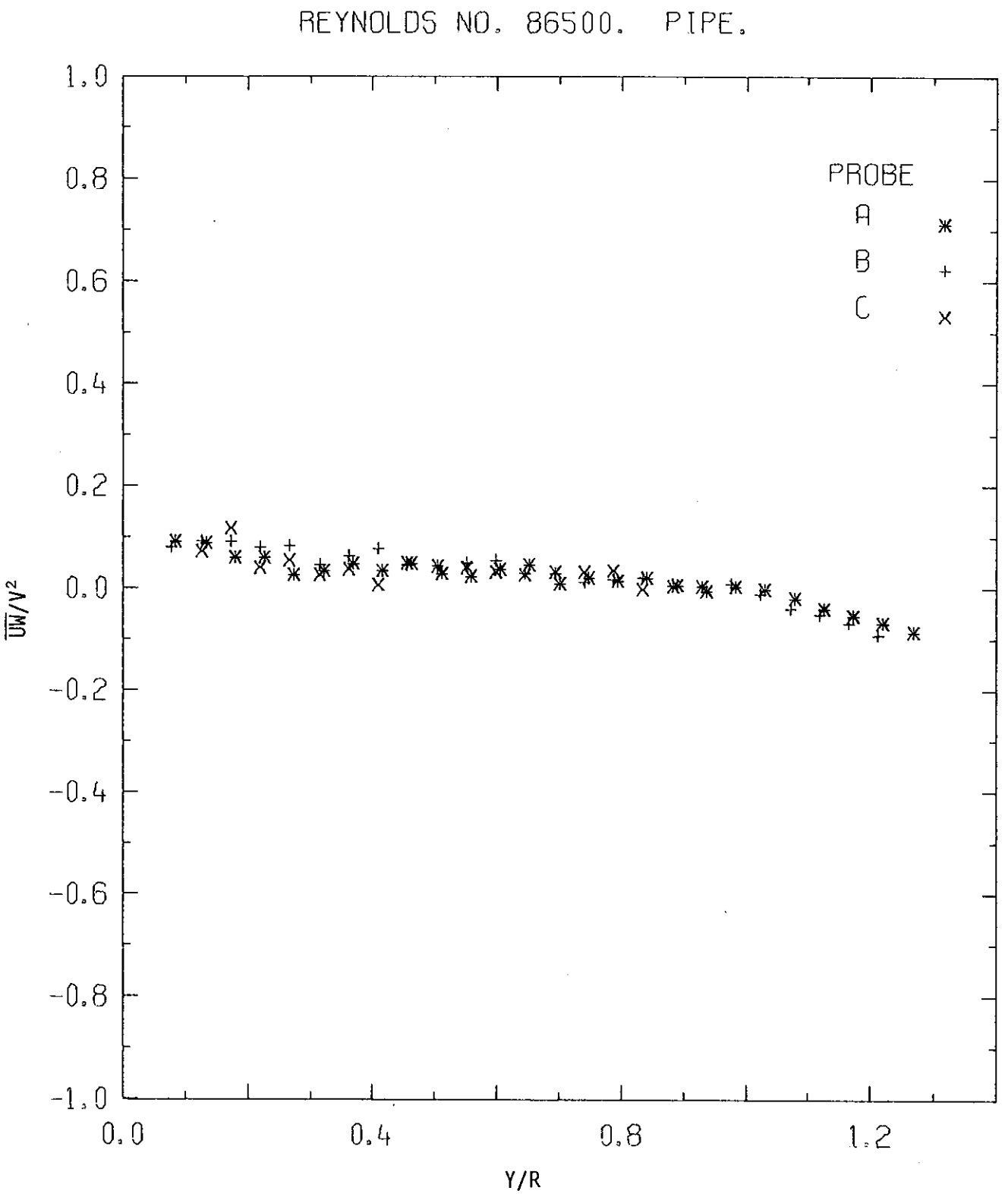

FIGURE 12(e). AZIMUTHAL COMPONENT OF REYNOLDS SHEAR STRESS, CALIBRATION PIPE 2

APPENDIX A
RESPONSE CORRELATION OF 5 μm DIAMETER 2 mm LONG TUNGSTEN-WIRE PROBE

The tabulated response of the standard ISVR 2 mm long x 5 μm diameter tungsten wire-probe is given in Table A1. The probe has a cold resistance of 7.5 ohms at 18°C, and the probe support prongs are separated from the active wire element by 1.5 mm of copper plating to minimise aerodynamic interference. The standard overheat resistance is 15 ohms for all probes, irrespective of the ± 10 per cent spread in the probe element resistance found during manufacture. Section 3.4 shows that the assumption of the similarity of the probe response to the standard curve is valid for a range of overheat ratios exceeding the resistance spread created by the probe manufacture.

A piecewise expansion about the operating velocity has been used to calculate the n exponent [Bruun 1971a, 1976b]:

$$n = \ell n \left[\frac{E_1^2 - E_0^2}{E_2^2 - E_0^2} \right] \Big/ \ell n \left[\frac{U_2}{U_1} \right] \qquad \text{(A1)}$$

The yaw exponent m was found by measurement of the $-\rho\ \overline{uv}$ component of the Reynolds stresses for axisymmetric pipe flow [Bruun and Davies 1969].

TABLE A1

STANDARD CALIBRATION OF A 2 mm, 5 μm DIAMETER TUNGSTEN HOT-WIRE PROBE OPERATED AT 15 Ω

Air temperature 18°C

Velocity U ($m\ s^{-1}$)	Bridge Output E (V)	Exponent n	Exponent m
0	1.167	-	-
0.2	1.269	-	-
0.4	1.336	0.72	-
0.6	1.387	0.65	-
0.8	1.425	0.60	-
1	1.457	0.56	0.51
1.2	1.486	0.54	0.50
1.4	1.511	0.53	0.50
1.6	1.533	0.52	0.49
1.8	1.554	0.52	0.49
2	1.570	0.515	0.48
2.5	1.611	0.510	0.48
3	1.648	0.505	0.465
3.5	1.681	0.505	0.460
4	1.711	0.500	0.455
5	1.764	0.500	0.445
6	1.810	0.495	0.440
7	1.852	0.490	0.435
8	1.889	0.490	0.430
9	1.923	0.485	0.425
10	1.955	0.485	0.420
12	2.012	0.480	0.415
14	2.062	0.480	0.415
16	2.108	0.475	0.410
18	2.149	0.470	0.405
20	2.187	0.465	0.400
25	2.270	0.460	0.395
30	2.341	0.450	0.390
35	2.405	0.445	0.385
40	2.458	0.440	0.380

(Continued)

Velocity U ($m\ s^{-1}$)	Bridge Output E (V)	Exponent n	Exponent m
45	2.509	0.430	0.380
50	2.553	0.425	0.375
60	2.632	0.415	0.375
70	2.702	0.405	-
80	2.761	0.400	-
90	2.814	0.390	-
100	2.862	0.385	-
110	2.906	0.375	-
120	2.946	0.370	-
130	2.982	0.365	-
140	3.017	0.360	-
150	3.049	0.360	-

APPENDIX B
SMALL-SIGNAL APPROXIMATION TO ANEMOMETER CORRELATION

Normal Wire

The steady-state correlation of a hot-wire element normal to the mean velocity U of a turbulent air stream is:

$$E^2 - E_0^2 = C\,B\,U^n \quad . \tag{B1}$$

Neglecting the turbulent velocity component, v, parallel to the wire gives

$$(E+e)^2 - E_0^2 = C\,B\,U^n \left[1 + \frac{nu}{U} + \frac{n}{2} + \left(\frac{u^2}{U^2} + \frac{w^2}{U^2}\right) + \frac{n}{2}\left(\frac{n}{2} - 1\right)\left(\frac{2u}{U} + \frac{u^2}{U^2} + \frac{w^2}{U^2}\right) + \cdots\right] . \tag{B2}$$

Subtracting the steady-state correlation, and neglecting second-order and higher terms of the Taylor's expansion,

$$2eE = (E^2 - E_0^2)\,\frac{n\,u}{U} \quad . \tag{B3}$$

Squaring and time averaging gives the axial component of the normal Reynolds stresses:

$$\overline{u^2} = \frac{4\,\overline{e^2}\,E^2\,U^2}{n^2(E^2-E_0^2)^2} \quad . \tag{B4}$$

The same result may be found by taking the partial derivative of Equation B1, $\left(\frac{\partial E}{\partial U}\right)$, and ignoring the velocity dependence of B and n.

Inclined Wire

The response of a wire inclined at an angle α between the normal to the wire and the incident velocity U is:

$$E_\alpha^2 - E_{0\alpha}^2 = C\ B\ U^n \cos^m \alpha \quad . \tag{B5}$$

The instantaneous angle of the velocity vector V to the wire normal β is given by:

$$\cos\beta = \frac{\underset{\sim}{V} \cdot \underset{\sim}{n}}{|\underset{\sim}{V}|} \quad .$$

$$= \cos\alpha \frac{(U+n + v\tan\alpha)}{|\underset{\sim}{V}|}$$

Expanding Equation (B5) for turbulent flow

$$(E_\alpha + e_\alpha)^2 - E_{0\alpha}^2 = C\ B |\underset{\sim}{V}|^n \cos^m \alpha \frac{[U+u + v\tan\alpha]^m}{|\underset{\sim}{V}|^m} \quad . \tag{B6}$$

Expanding Equation B6 by a Taylor's series:

$$E_\alpha^2 + 2e_\alpha E_\alpha + E_\alpha^2 - E_{0\alpha}^2 = C\ B\ U^n \cos^m \alpha \cdot [1 + (n-m)\frac{u}{U} + \frac{n-m}{2} \cdot$$

$$\cdot \frac{1}{U^2}(n^2+v^2+w^2) + (\frac{n-m}{2}) \cdot (\frac{n-m-2}{2}) \cdot$$

$$\cdot (\frac{2u}{U} + \frac{1}{U^2}(u^2+v^2+w^2))^2 + \ldots] \cdot$$

$$\cdot [1 + m(\frac{u}{U} + v\frac{\tan\alpha}{U}) + \ldots] \quad .$$

Neglecting terms of the second order or higher, and subtracting Equation B5,

$$\frac{2\ e_\alpha E_\alpha}{(E_\alpha^2 - E_{0\alpha}^2)} = \frac{n}{U}(u + \frac{m}{n}\tan\alpha\ v) \quad . \tag{B7}$$

Both the normal and inclined wire small-signal response equations are independent of the ratio C to the standard probe response to the first-order approximations. If the inclined wire is rotated by 180° about its axis, the sign of the v component of Equation B7 changes. Squaring and time averaging this equation at positions 1 and 5 of the standard rotation sequence (Figure 10(b)) leads to $\rho\ \overline{v^2}$ and $\rho\ \overline{uv}$, after determination of $\rho\ \overline{u^2}$ by Equation B4. The rotation of the probe about the duct and probe axis can best be described by matrix transforms of the coordinate system. The transformed coordinate system A_T is related to the earlier A by

$$A_T = L' A L \quad , \tag{B8}$$

where L is for the rotation about only one axis

$$L = \begin{bmatrix} 1 & 0 & 0 \\ 0 & \ell_2{}'_2 & \ell_2{}'_3 \\ 0 & \ell_3{}'_2 & \ell_3{}'_3 \end{bmatrix} \tag{B9}$$

The components of L, ($\ell_2{}'_3$ etc.), are the direction cosines of the new axis to the old, and L' is the inverse of L.

The coordinate system used to resolve the six terms of the Reynolds stress tensor are arbitrary. The inclined wire signal variance at locations 2 and 4 on the standard rotation sequence of Figure 10(b) was used to form two independent estimates of $-\rho\ \overline{vw}$ in terms of the orthogonal coordinates defined by the rig axis and positions 1 and 3.

APPENDIX C
ERROR ESTIMATION ON REYNOLDS STRESSES AND P RATIO

The small-signal approximations to the hot-wire equations are assumed to be exact for this error analysis, which therefore ignores the further errors created by the higher order terms of the Taylor's series expansion. The measurement errors are also assumed to be statistically independent. The standard deviation σ of the determination of function f is:

$$\sigma^2 = \sum_{i=1}^{q} \left(\frac{\partial f}{\partial x_i} \right)^2 \sigma_i^2 \qquad \text{(C1)}$$

The parameters x_i, q in number, are each subject to an estimated or assumed standard deviation σ_i. The parameters x_i and the associated standard deviation σ_i are given in Table C1.

TABLE C1

Parameter x_i	$\pm \sigma_i$ %
Mean velocity U	1.0
Bridge voltage (no flow)	1.0
Bridge voltage (flow)	0.1
m index	1
n index	1
Signal variance	1
Inclined wire angle α	0.5°

The same error estimation applies to the P ratio (Section 3.5), or the ratio of the measured to calculated signal cross product $\overline{e_\alpha e}$. The error estimation results for the Reynolds stresses and the P ratio are given by Table C2.

TABLE C2

Study	$\rho \overline{u^2}$ ± %	$-\rho \overline{v^2}$ ± %	$-\rho \overline{uv}$ ± %	$-\rho \overline{vw}$ ± %	P ± %
Present	6	20	10	100	5
Champagne and Sleicher ($u'/U < 0.2$)	5	15	12	-	-
Riberio and Whitelaw ($k/U^2 = 0.8$)		4	17	6	-

The error estimation is thus in general agreement with that of Champagne and Sleicher [1967] and Riberio and Whitelaw [1976]. The failure of the small-signal approximations in higher turbulence intensity flows may be readily detected by the increasing divergence of the P ratio from unity.

References

Champagne, F.H. and Schleicher, C.A. [1967] - Turbulence measurements with inclined hot wires. Part 2 - Hot-wire response equations. J. Fluid Mech., Vol.28, No.1, p.177.

Riberio, M.M. and Whitelaw, J.H.. [1976] - Turbulent mixing of co-axial jets with particular reference to the near exit region. Trans. ASME, Ser. I, Vol.98, No.21, p.284.